Dual neofunctionalization of a rapidly evolving aquaporin-1 paralog resulted in constrained and relaxed traits controlling channel function during meiosis resumption in teleosts

Cinta Zapater,[1] François Chauvigné,[1] Birgitta Norberg,[2] Roderick Nigel Finn,[3,4] and Joan Cerdà*,[1]

[1]Laboratory of Institut de Recerca i Tecnologia Agroalimentàries (IRTA)-Institut de Ciències del Mar, Consejo Superior de Investigaciones Científicas (CSIC), 08003 Barcelona, Spain

[2]Institute of Marine Research, Austevoll Research Station, Institute of Marine Research, 5392 Storebø, Norway

[3]Department of Biology, University of Bergen, Bergen High Technology Centre, N-5020 Bergen, Norway

[4]Institute of Marine Research, PO Box 1870 Nordnes, 5005 Bergen, Norway

***Corresponding author:** E-mail: joan.cerda@irta.cat

This submission is intended as a Research Article

Short running title: Adaptive evolution of teleost Aqp1 paralogs

Key words: Aquaporin, Oocyte, Meiosis, Hydration, Yolk, Neofunctionalization

List of non-standard abbreviations:

Aqp - aquaporin; EH - early hydrating oocyte; H - hydrated oocytes; LG - linkage group; MH - mid-hydrated oocytes; PV - post vitellogenic follicles; Vtg - vitellogenin; WGD - whole genome duplication

Abstract

The pre-ovulatory hydration of marine teleost oocytes is a unique process among vertebrates. The hydration mechanism is most pronounced in modern acanthomorph teleosts that spawn pelagic (floating) eggs, however the molecular pathway for water influx remains poorly understood. Recently, we revealed that whole genome duplication (WGD) resulted in teleosts harbouring the largest repertoire of molecular water channels in the vertebrate lineage, and that a duplicated aquaporin-1 paralog is implicated in the oocyte hydration process. However, the origin and function of the aquaporin-1 paralogs remains equivocal. By integrating the molecular phylogeny with synteny and structural analyses we show here that the teleost *aqp1aa* and *-1ab* paralogs (previously annotated as *aqp1a* and *-1b*, respectively) arose by tandem duplication rather than WGD, and that the Aqp1ab C-terminus is the most rapidly evolving subdomain within the vertebrate aquaporin superfamily. The functional role of Aqp1ab was investigated in Atlantic halibut, a marine acanthomorph teleost that spawns one of the largest pelagic eggs known. We demonstrate that Aqp1ab is required for full hydration of oocytes undergoing meiotic maturation. We further show that the rapid structural divergence of the C-terminal regulatory domain causes ex vivo loss of function of halibut Aqp1ab when expressed in amphibian oocytes, but not in zebrafish or native oocytes. However, by using chimeric constructs of halibut Aqp1aa and -1ab, and antisera specifically raised against the C-terminus of Aqp1ab, we found that this cytoplasmic domain regulates *in vivo* trafficking to the microvillar portion of the oocyte plasma membrane when intra-oocytic osmotic pressure is at a maximum. Interestingly, by co-injecting polyA$^+$ mRNA from post-vitellogenic halibut follicles, *ex vivo* intracellular trafficking of Aqp1ab is rescued in amphibian oocytes. These data reveal that the physiological role of Aqp1ab during meiosis resumption is conserved in teleosts, but the remarkable degeneracy of the cytoplasmic domain has resulted in alternative regulation of the trafficking mechanism.

Introduction

Meiosis resumption is a ubiquitious developmental feature of vertebrate oocytes, in which the germinal vesicle matures in preparation for fertilization (Eppig et al. 2004; Philpott and Yew 2008; Lessman 2009). In oviparous marine teleosts, however, meiosis resumption is synchronized with the cytoplasmic enlargement of the oocyte as a result of a massive water uptake (Fulton 1898). This process of oocyte hydration evolved exclusively in the teleost lineage and is thus unique among vertebrates. It is found in ancient elopomorph, clupeimorph and modern acanthomorph teleosts and represents a pre-adaptation to the oceanic environment since it assures a water reservoir when single-celled eggs are released into the hyperosmotic seawater (Fyhn et al. 1999; Finn and Kristoffersen 2007). The degree of hydration, however, appears to vary according to the system of intracellular osmolyte generation. Available evidence suggests that species that spawn benthic (sinking) eggs predominantly accumulate inorganic ions such as K^+, Cl^-, PO_4^{3-} or Na^+ (Greeley et al. 1991; Cerdà et al. 2007; Kristoffersen and Finn 2008), while those that spawn pelagic (floating) eggs further activate lysosomal proteases (cathepsins) that differentially degrade vitellogenin (Vtg)-derived yolk proteins to generate an additional organic osmolyte pool of free amino acids (FAA) (Cerdà et al. 2007; Finn and Fyhn 2010). The innate stimuli that activate these processes are C_{21} steroids (progestins) synthesized by the granulosa cells in response to a surge of luteinizing hormone secreted by the pituitary (Thomas et al. 2007; Nagahama and Yamashita, 2008). This endocrine cascade initiates meiosis resumption, cytoplasmic maturation, and the accumulation of osmolytes for oocyte hydration (Cerdà et al., 2007; Thomas et al. 2007; Nagahama and Yamashita, 2008). The interesting aspect is the positive selection of these latter mechanisms in modern acanthomorph teleosts. Regardless of systematic affinities or ecological niche, the majority of extant marine acanthomorph teleosts depolymerise VtgAa-type yolk proteins and spawn pelagic eggs (Cerdà et al. 2007; Finn and Kristoffersen 2007; Finn 2007ab; Kolarevic et al. 2008). Consequently, the phenotypic nature of the pelagic egg, which facilitates oxygen exchange and dispersal of the early embryos in the ocean, has been associated with the remarkable radiation of teleosts during the Eocene (Fyhn et al. 1999; Finn and Kristoffersen 2007).

For many years it was thought that the pathway for water entry into the maturing teleost oocyte was benign, occurring via bulk flow across the plasma membrane. However, the short temporal phase of the hydration process suggested that a specific mechanism must have co-evolved to facilitate the controlled movement of water into the oocyte. In line with this hypothesis, we recently identified a teleost-specific ortholog of the mammalian aquaporin-1 water channel (Fabra et al. 2005). This novel aquaporin (Aqp1ab, previously named Aqp1o or Aqp1b) is the channel most likely involved in oocyte hydration (Fabra et al. 2005, 2006; Tingaud-Sequeira et al. 2008). In the perciform teleost gilthead seabream (*Sparus aurata*), which produces pelagic eggs, Aqp1ab is synthesized in early oocytes and transported towards the oocyte cortex throughout the growth period (Fabra et al. 2006). Aqp1ab has also been implicated in oocyte hydration of other species, where high ovarian *aqp1ab* expression is found in marine and catadromous teleosts producing pelagic eggs (Tingaud-Sequeira et al. 2008; Sun et al. 2009, 2010). Interestingly, *aqp1ab* transcripts are also highly accumulated in the ovary of some freshwater species, such as the stinging catfish (*Heteropneustes fossilis*), in which oocytes partially hydrate during meiotic maturation although benthic eggs are produced (Chaube et al. 2011).

In addition to circumstantial evidence (i.e., specific subcellular localization of Aqp1ab in the oocyte correlating with the hydration process), the physiological role of Aqp1ab is supported by the observation that the swelling of oocytes undergoing meiosis resumption is completely or partially blocked by aquaporin inhibitors such as mercury and tetraethylammonium (Fabra et al. 2005, 2006; Kagawa et al. 2009). However, it is known that these compounds can also affect K^+ channels and other ion transport proteins (Armstrong 1990; Jacoby et al. 1999), which may play a role for inorganic osmolyte accumulation in the oocyte (Cerdà et al. 2007; Kristoffersen and Finn 2008). Therefore, direct evidence for the role of Aqp1ab during fish oocyte hydration is still lacking. In addition, while the majority of teleost aquaporins appear to have arisen as a consequence of whole genome duplication (WGD) (Tingaud-Sequeira et al. 2010), the *aqp1aa* and *-1ab* genes were suggested to be the result of tandem duplication (Tingaud-Sequeira et al. 2008). To address these issues, we selected the Atlantic halibut (*Hippoglossus hippoglossus*) as an experimental model, since it is a marine acanthomorph teleost that reproduces at low temperature and spawns one of the largest pelagic eggs known. We isolated two novel

aquaporin-1 transcripts and examined the functional role of Aqp1ab during meiosis resumption using *ex vivo* and *in vivo* approaches. To determine the duplication history of the teleost *aqp1aa* and *-1ab* genes, we re-examined the molecular phylogeny of the transcripts and deduced proteins in relation to 26 vertebrate orders. These data revealed that tetrapod *AQP1* and teleost *aqp1aa* orthologs have experienced purifying selection within each clade, while the teleost *aqp1ab* orthologs displayed a paralogous subclustering topology. To determine whether a given subcluster could represent the product of WGD, an extended synteny analysis was performed for selected tetrapod and teleost genomes.

Materials and Methods

Animals and Sample Collection

Adult and juvenile Atlantic halibut were kept in circular tanks of 7 m in diameter at 5-6ºC in filtered seawater (35‰ salinity) at the Austevoll Research Station (Institute of Marine Research, Norway). Tissue samples were dissected from sacrificed juvenile fish, frozen in liquid nitrogen and stored at -80ºC until analysis. Ovarian biopsies were taken weekly from adult females that had reached stable ovulatory rhythms, in connection with regular checking of maturity status of broodstock (Norberg et al. 1991; Finn et al. 2002). Biopsies containing ovarian follicles at different developmental stage and unfertilized eggs were collected from adult females by using 4-mm diameter silicone tubes introduced in the ovipore and attached to 10 ml syringes. Ovarian follicles were immediately placed in 75% Leibovitz L-15 medium with L-glutamine (Sigma-Aldrich, Madrid, Spain) and 100 µg gentamicin/ml, pH 7.5 (Selman and Wallace 1986), and classified into different stages depending on the extent of oocyte hydration: follicles containing postvitellogenic, non hydrated oocytes (PV), follicles with early hydrating oocytes (EH), follicles with mid-hydrated oocytes (MH), follicles with hydrated oocytes (H), and ovulated oocytes or unfertilized eggs (Egg). Some of the PV and EH ovarian follicles were used for microinjection and *in vitro* incubations; the other follicles were frozen in liquid nitrogen and stored at -80ºC. Adult zebrafish were obtained from a local pet store and maintained as described by Westerfield (1995). Procedures related to the care and use of fish followed the

International Guiding Principles for Biomedical Research Involving Animals as promulgated by the Society for the Study of Reproduction.

Cloning and Sequencing of Atlantic halibut Aquaporin-1aa and -1ab

Full-length Atlantic halibut aquaporin-1a (*hhaqp1aa*) and -1b (*hhaqp1ab*) cDNAs were isolated by RT-PCR. Total RNA was extracted from the intestine using the RNAeasy Minikit (Qiagen GmbH, Hilden, Germany), and 10 µg were reverse transcribed using 0.5 µg oligo-$(dT)_{17}$, 1 mM dNTPs, 40 IU RNAse inhibitor (Roche, Barcelona, Spain), and 10 IU SuperScript II (Invitrogen, Barcelona, Spain), for 1.5 h at 42ºC. A partial cDNA encoding *hhaqp1aa* was isolated by RT-PCR using degenerate oligonucleotide primers (F = 5'-GACCAGGARRTSAAGGTG-3' and R = 5'-CACATVGGCCCSACCCAG-3') designed to regions close to the two highly conserved Asn-Pro-Ala (NPA) motifs of teleost Aqp1aa (Tingaud-Sequeira et al. 2008). The sequence obtained was used to design specific primers to isolate the 5' and 3' ends by RACE kits (Invitrogen). For the 5' end, the two reverse primers were 5'-AGCAACTGGGCCACAATGTA-3' and 5'-CGCTGATGTGGCCTAAACTC-3', and the 3' end the forward primers were 5'-AACCTTCCAGCTGGTGCTGT-3', and 5'-GTCCGGCTTTGATCCTGAAC-3'. The full-length *hhaqp1aa* cDNA was finally amplified with the 3' RACE kit (Invitrogen) using a forward (5'-TTTAGAGAGGACCAGCTCAAACC-3') and AUAP primers and a high fidelity polymerase (Easy-A™ High-Fidelity PCR Cloning Enzyme; Stratagene, Cultek SLU, Madrid, Spain). The products were cloned into the pGEM-T Easy vector (Promega Biotech Iberica SL, Madrid, Spain) and sequenced with BigDye Terminator version 3.1 in DNA analyzer ABI PRISM 377 (Applied Biosystems, Madrid, Spain). For the cloning of the *hhaqp1ab* cDNA, 10 µg of total RNA extracted from H ovarian follicles were used for reverse transcription as indicated above. The 3' RACE kit was used to amplify the full-length cDNA using a specific forward primer designed from an available expressed sequence tag (EST; GenBank accession no. EB039821), 5'-GTTTAAACAGACTCCCCAAAAC-3', and the AUAP primer. The PCR products were cloned and sequenced as above. The nucleotide sequences of full-length *hhaqp1aa* and -*1ab* cDNAs were submitted to the DDBJ/EMBL/GenBank database under the accession numbers HQ185294 and HQ185295, respectively.

Phylogenetic Analyses

Molecular phylogenies of the cloned aquaporin transcripts and deduced proteins were analyzed via Bayesian (Mr Bayes v3.1.2) and Maximum likelihood protocols as described previously (Finn and Kristoffersen 2007). Aqp1 orthologs and ESTs (see supplementary table S1, Supplementary Material online) were obtained from public databases (Ensembl and GenBank) and multiple sequence alignments constructed using the T-coffee suite of alignment tools (Notredame et al. 2000). Each amino acid alignment was converted to a codon alignment (nucleotide triplets) via PAL2NAL (Suyama et al. 2006) and then manually adjusted to correct for errors using MacVector (MacVector Inc, Cambridge, UK). For Bayesian analyses the following models were tested for the codon alignments: nucmodel = 4by4 with nst = 2 or codon with nst = 6; rates = gamma and invgamma, respectively; and for amino acid alignments: aamodel = mixed. For all alignments, MCMC algorithms were run with 1 and 5 million generations using 3 heated chains and 1 cold chain. All runs were examined for convergence using Tracer version 1.5 (www.beast.bio.ed.ac.uk/Tracer), and majority rule consensus trees summarized with a burnin of 3,500.

To validate the inferred tree topologies, syntenic analyses were performed for selected teleost and tetrapod genomes using ensembl v62 and Genomicus v62.01 as described previously (Chauvigné et al. 2010). Three-dimensional models of HhAqp1aa and -1ab were reconstructed using ModWeb (www.modbase.compbio.ucsf.edu) to evaluate the putative folding of the C-terminal domains, while overall tertiary structure was compared to crystallographic data available for human (1H6I) and bull (1J4N) AQP1. Predicted phosphorylation sites were searched using the online NetPhos and NetPhosK servers (www.cbs.dtu.dk) according to Blom et al. (1999, 2004).

Real-time Quantitative PCR

The expression pattern of *hhaqp1aa* and *-1ab* in different adult tissues of Atlantic halibut, as well as in hydrating ovarian follicles and unfertilized eggs, was determined by quantitative real-time PCR (qPCR). Total RNA was extracted with the RNAeasy Minikit (Qiagen), treated with DNase I using RNase-Free DNase kit (Qiagen), and 0.5 μg reverse

transcribed as indicated above. Real-time quantitative PCR (qPCR) amplifications were performed using SYBR Green qPCR master mix (Applied Biosystems) on 2 µl of diluted (1:10) cDNA as described previously (Chauvigné et al. 2010). Primers representing the 3'-end of each aquaporin open reading frame were used to amplify products for *hhaqp1aa* (262 bp using F = 5'-GTCCGGCTTTGATCCTGAAC-3' with R = 5'-CAGGAGTATGGACACGTGCAG-3') and *hhaqp1ab* (174 bp using F = 5'-CCGGCGGTTATACTGGAGTC-3' with R = 5'-AGTGTCAGTGTCCGCTGAGG-3'), and cycle numbers were normalized to 18S ribosomal RNA (149 bp using F = 5'-GAATTGACGGAAGGGCACCACCAG-3' with R = 5'-ACTAAGAACGGCCATGCACCACCAC-3') or β-actin (643 bp using F = 5'-ACATGGAGAAGATCTGGC-3' with R = 5'- GCGTACAGGTCCTTACGGA-3'). The sequences were amplified in duplicate for each sample on 384-well plates using the ABI PRISM 7900HT sequence detection system (Applied Biosystems). The relative transcript level was calculated by using a standard curve generated for each primer pair from 10-fold serial dilutions of a pool of first-stranded cDNA template from ovary samples. All calibration curves exhibited correlation coefficients higher than 0.98, and the corresponding qPCR efficiencies were greater than 99%. Changes in *hhaqp1ab* expression in hydrating ovarian follicles were determined as fold change with respect the PV follicles using the $2^{-\Delta\Delta Ct}$ method (Livak et al. 2001).

Production of HhAqp1b Polyclonal Antiserum

Antiserum was raised in rabbits against a synthetic peptide corresponding to amino acid residues 255 to 267 (C-terminus) of HhAqp1ab with the predicted initiation codon (methionine, ATG) designated as residue 1 (Agrisera AB, Sweden). Affinity purification was accomplished against the synthetic peptide immobilized using UltraLinkTM Iodoacetyl resin (Pierce, Rockford, IL, USA) according to manufacturer instructions. Bound IgG was eluted with acidic 100 mM glycine (pH 2.5) into fourfold excess 1 M Tris (pH 9), and precipitated using saturated ammonium sulfate solution. The pellet was resuspended in sterile PBS (pH 7.4) and buffer exchanged to PBS (pH 7.4) using PD-10 Desalting columns (Amersham Biosciences Ab, Uppsala, Sweden).

Expression Constructs

Wild-type *hhaqp1aa* and *-1ab* full-length cDNAs were cloned into the *Eco*RV/*Spe*I sites of the oocyte expression vector pT7Ts (Deen et al. 1994). The cDNAs encoding *hhaqp1aa* and *-1ab* chimeras, where the N- and C-terminus were interchanged, were synthesized by Mr Gene GmbH (Germany) and subcloned into the pT7Ts vector (see supplementary table S2, Supplementary Material online). Sequence analysis of the clones in pT7Ts was carried out to confirm that the desired chimeras were produced.

Functional Expression in Fish and Amphibian Oocytes

Complementary RNAs (cRNAs) were synthesized as described (Deen et al. 1994) and microinjected *in vivo* into PV oocytes of Atlantic halibut, and *ex vivo* into oocytes of the African clawed frog (*Xenopus laevis*) and zebrafish (*Danio rerio*).

African clawed frog

Isolation, defolliculation and injection of *X. laevis* stage V-VI oocytes were performed essentially as described previously (Deen et al. 1994). Oocytes were injected with 50 nl of water alone (controls) or containing 1 or 25 ng of *hhaqp1aa* and *-1ab* cRNA, respectively. In some experiments, oocytes were injected with 25 nl water with or without 50 ng of polyA$^+$ mRNA purified from PV and EH halibut ovarian follicles, or with 25 nl of water containing 25 ng of *hhaqp1ab* cRNA with or without 50 ng mRNA. Subsequently, *hhaqp1ab* and mRNA-injected oocytes were injected again with PBS alone or containing 100, 250 or 500 ng of affinity-purified HhAqp1ab antiserum or rabbit IgG (Sigma-Aldrich; controls) in a volume of 25 nl. The polyA$^+$ mRNA was purified from total RNA using the Oligotex mRNA Mini Kit (Qiagen). The osmotic water permeability (P_f) was measured from the time course of oocyte swelling in a standard assay 48 h after injections. Oocytes were transferred from 200 mOsm modified Barth's culture medium (MBS; 0.33 mM $Ca(NO_3)_2$, 0.4 mM $CaCl_2$, 88 mM NaCl, 1 mM KCl, 2.4 mM $NaHCO_3$, 10 mM Hepes, 0.82 mM $MgSO_4$, pH 7.5) to 20 mOsm MBS at room temperature. Oocyte swelling was followed by video microscopy using serial images at 2 s intervals during the first 20 s period, and P_f values were calculated from the time-course changes in relative oocyte volume as described (Deen et al. 1994). To examine the effect of mercury on P_f, injected

oocytes were incubated in MBS containing 0.3 mM $HgCl_2$ for 15 min before and during the swelling assays. The reversibility of the mercury inhibition was determined by rinsing the same oocytes three times with fresh medium, and further incubation with 5 mM β-mercaptoethanol for 15 min prior to the swelling assays.

Atlantic halibut

For *in vivo* expression of HhAqp1aa and -1ab in PV Atlantic halibut oocytes (1.8 mm diameter), the selection, injection and defolliculation of oocytes, as well as the swelling assays, were performed at 4-6ºC. Healthy ovarian follicles were selected from the ovarian biopsies, and after equilibration for approximately 4 h in L-15 medium, follicle-enclosed oocytes were injected with 50 nl of water or *hhaqp1aa* and *-1ab* cRNAs as indicated above. After 24 h in fresh L-15 medium, oocytes were partially defolliculated using watchmaker forceps, and subjected to the swelling assays 24 h later. For the determination of the P_f values, oocytes were transferred to 10-fold diluted L-15 medium (30 mOsm), and the diameter of the oocytes was measured under a stereomicroscope at 5 s intervals during the first 50 s period. The effect of mercury on the P_f and its reversibility with β-mercaptoethanol was tested as in *X. laevis* oocytes.

Zebrafish

Females were sedated by immersion for approximately 15 min in 100 ppm phenoxyethanol, sacrificed by decapitation, and ovaries immediately placed in modified Cortland's culture medium without calcium and magnesium (0.124 M NaCl, 0.006 M $NaHCO_3$, 0.003 M Na_2HPO_4, 0.005 M KCl, 5 g Hepes, 0.03 g penicillin, 0.05 g streptomycin, pH 7.8). Ovarian follicles containing fully-grown oocytes (0.5-0.6 mm diameter) were manually dissected from the ovary, transferred into fresh culture medium, and after equilibration for 2-4 h at 26ºC, were injected with 5 nl of water or containing 9 ng of *hhaqp1aa* or *-1ab* cRNA. Follicles were then incubated for 12-16 h at 26ºC. The P_f measurements were performed as above but under hypertonic conditions using Cortland's with 150 mM sucrose (400 mOsm), since oocytes became slightly translucent after exposure to 10-fold diluted Cortland's. Treatment of follicles with mercury and β-mercaptoethanol was carried as above.

Inhibition of Atlantic halibut Oocyte Hydration with $HgCl_2$ and HhAqp1ab Antiserum

To test the effect of mercury on oocyte hydration, EH ovarian follicles were separated from the ovarian biopsies and kept in L-15 medium at 4ºC. After 2 h of equilibration, follicles were exposed to increasing doses of $HgCl_2$ (0.25, 0.5 or 1 mM) for 30 min, washed with fresh medium, and subsequently treated or not with 5 mM β-mercaptoethanol for another 30 min. The effect of the HhAqp1ab antiserum was studied by injecting EH follicles with PBS vehicle or with increasing doses of HhAqp1ab antibody or rabbit IgG (100, 200, 250 or 500 ng/oocyte) in a volume of 50 nl. Additionally, a fraction of the follicles injected with 200 ng of anti-HhAqp1ab antibody were co-injected with 50 nl of water containing 25 ng of *hhaqp1aa* or *-1ab* cRNA. In all cases, follicles were transferred to fresh L-15 medium and incubated at 4-5ºC for 48-72 h to resume meiotic maturation and hydration *in vitro*. The diameter of the ovarian follicles was measured before and after the incubation period. Follicle samples from all the treatments were frozen at -80ºC for further analyses.

SDS-PAGE of Oocyte Yolk Proteins

Halibut ovarian follicles with oocytes at different stages during meiotic maturation and hydration were mechanically homogenized in 1 x Laemmli sample buffer (Laemmli 1970) and denatured at 95°C for 5 min. A volume corresponding to 0.02 oocyte equivalents was loaded in each lane for yolk protein profile determination. SDS-PAGE was performed in 12% acrylamide minigels (7 x 3 x 10 cm) and electrophoresed at constant voltage (130 V) for 1.5 h. After fixation in 12.5% trichloroacetic acid during 1 h at room temperature, the gel was stained overnight in 0.2% PlusOne Coomassie Blue PhastGel R-350 (GE Healthcare, Barcelona, Spain) in 30% methanol and 10% acetic acid solution. The gel was progressively destained in 25% methanol and 7% acetic acid solution until the bands were clearly revealed.

Membrane Isolation and Immunoblotting

X. laevis oocytes, and Atlantic halibut ovarian follicles and adult tissues, were homogenized in HbA buffer [20 mM Tris pH 7.4, 5 mM $MgCl_2$, 5 mM NaH_2PO_4, 1 mM

EDTA, 80 mM sucrose, and cocktail of protease inhibitors (Mini EDTA-free, Roche)], and centrifuged twice at 200 x *g* for 5 min at 4ºC. Total membranes were isolated by a final 20 min centrifugation at 13000 x *g* at 4ºC and resuspended in 1 x Laemmli sample buffer. Alternatively, membranes were solubilized in PBS (pH 7.5) containing 0.5% SDS and protease inhibitors, and protein concentration was measured using the Bio-Rad Protein Assay kit (Bio-Rad Laboratories Inc, Madrid, Spain). Plasma membranes were isolated from *X. laevis* oocytes as described (Kamsteeg and Deen 2001). Whole homogenates were prepared by homogenizing the ovarian follicles directly in 1 x Laemmli sample buffer.

For immunoblotting, one volume of protein extract equivalent to 0.5-5 oocytes or ovarian follicles, or 30-60 µg protein for tissues, was denatured at 95ºC for 10 min, and subjected to 12% SDS-PAGE. After electrophoresis, the proteins were transferred onto nitrocellulose membranes (GE Healthcare) with Tris-glycine-methanol buffer (190 mM glycine, 250 mM Tris pH 8.6, and 20% methanol). The membranes were blocked for 1 h at room temperature in TBST (20 mM Tris, 140 mM NaCl, 0.1% Tween, pH 7.6) with 5% non-fat milk powder, and subsequently incubated with the HhAqp1ab antiserum (1:500) overnight at 4ºC. Control membranes were incubated with the HhAqp1ab antiserum pre-adsorbed with a 30-fold molar excess of the immunizing peptide. Bound antibodies were detected with 1:2000-diluted goat anti-rabbit IgG (Rockland, Tebu-bio, Barcelona, Spain) coupled to horseradish peroxidase (HRP), and proteins were visualized by using enhanced chemiluminescence (ECL; Picomax, Rockland). In some experiments, membranes were incubated only with goat anti-rabbit IgG-HRP (1:2000), or with the HhAqp1ab antiserum labelled with HRP (1:100) using the Lightning-Link^{TM} HRP Conjugation kit (Innova Biosciences, Antibody Bcn S.L, Barcelona, Spain), before ECL revelation. Finally, to investigate the possible glycosylation of HhAqp1ab, total membrane homogenates were treated with 500 U of N-Glycosidase F (PNGase F; New England Biolabs, Izasa, Barcelona, Spain) or 80 KU of Endo-α-N-Acetylgalactosaminidase (O-Glycosidase; New England Biolabs) following the manufacturer instructions prior to electrophoresis. Zebrafish aquaporin-3b (Tingaud-Sequeira et al. 2010) and fetuin (Sigma-Aldrich) were used as a positive controls for PNGase F and O-Glycosidase digestion, respectively.

Immunofluorescence Microscopy

Immunofluorescence localization was performed on paraffin embedded ovarian follicles and oocytes fixed with 4% paraformaldehyde (PFA) overnight at 4ºC. Sections of approximately 6 μm in thickness were blocked with 5% goat serum in PBST (0.1% BSA, 0.1% Tween in PBS) for 1 h, and incubated with anti-HhAqp1ab antibody (1:50 or 1:100) diluted in PBST with 1% goat serum overnight at 4°C. After washing with PBS, sections were incubated with FITC anti-rabbit secondary antibodies (Sigma-Aldrich; 1:300) diluted in PBS for 1 h, washed again with PBS, and incubated 3 min with 1:3000-diluted 4',6-diamidino-2-phenylindole (DAPI; Sigma-Aldrich). Controls were incubated with pre-adsorbed HhAqp1ab antiserum as described above. Sections were mounted with Fluoromount^{TM} aqueous mounting medium (Sigma-Aldrich), and immunofluorescence was observed and documented with a Zeiss imager.z1 microscope (Carl Zeiss MicroImaging, S.L., Barcelona, Spain).

Immunoelectron Microscopy

Atlantic halibut PV, EH and LH ovarian follicles collected from the biopsies were fixed in 4% PFA with or without 0.05% glutaraldehyde overnight at 4ºC, transferred to 2% PFA, and processed for immunoelectron microscopy as described previously (Fabra et al. 2006). The sections were blocked in 0.1 M PBS (pH 7.4) with 1% goat serum and 20 mM glycine for 30 min at room temperature, and subsequently incubated with the same buffer containing HhAqp1ab antisera (1:50) overnight at 4°C. After washing, the sections were incubated with protein A-coupled to gold particles (15 nm) in 1% goat serum, 20 mM glycine in PBS for 1 h at room temperature, washed, and contrasted with 2% uranil acetate for 15 min and lead citrate for 5 min. The images were documented and photographed by using a JEOL EM 1010 electron microscope (JEOL, Izasa, Barcelona, Spain).

Statistical Analysis

Data are the mean ± SEM and were statistically analyzed using one-way ANOVA followed by Tukey's pairwise comparison with a 95% confidence interval, or by the Student's *t*-test comparing experimental sets against control only. Percentage data that fell between the ranges of 0-20% or 80-100% were square root transformed prior to statistical analyses. Criteria for significant differences were at $p < 0.05$ for all comparisons.

Results

The Duality of Aquaporin-1 Water Channels in Teleosts

By using available EST sequence information and degenerate oligonucleotide primers, full-length cDNAs encoding *hhaqp1aa* and *-1ab* were isolated, confirming the expression of two Aqp1-like channels in Atlantic halibut as reported for other teleosts (Tingaud-Sequeira et al. 2008, 2010). Their open reading frames were 54.1% identical at the amino acid level, with 42.9% and 17.4% identity between the N- and C-terminal cytoplasmic sequences, respectively. Both HhAqp1aa and -1ab deduced amino acid sequences showed the six transmembrane helices and the two Asn-Pro-Ala (NPA) motifs which are typical features of the members of the aquaporin superfamily (see supplementary fig. S1, Supplementary Material online). In addition, both sequences had the residues forming the aromatic residue/arginine (ar/R) constriction region that are conserved in water-selective aquaporins (Phe^{50}, His^{172} and Arg^{187}, and Phe^{50}, His^{171} and Arg^{186}, in HhAqp1aa and -1ab, respectively), as well as a Cys residue close to the second NPA motif (Cys^{181} and Cys^{180}, in HhAqp1aa and -1ab, respectively), the site potentially responsible for the blockage of the water pore by mercury (Preston et al. 1993; Hirano et al. 2010).

The molecular phylogeny of the full length cloned transcripts and deduced amino acids was examined in relation to 26 vertebrate orders. All methods of inference revealed three sister clusters with robust separation of sarcopterygian (lungfish and tetrapod) AQP1 from the teleost Aqp1aa and -1ab orthologs (fig. 1). Addition of the zebrafish Aqp5/1b, apparently a pseudogene (Tingaud-Sequeira et al. 2010), produced some trees where it clustered basal to African lungfish Aqp1, but more often as an ancestral node to the teleost Aqp1aa and -1ab sequences. This putative pseudogene is therefore drawn as a polytomy between the sarcopterygian and actinopterygian orthologs. Higher resolution was achieved from the codon alignments, while amino acid alignments generated some polytomies (Bayesian posterior probabilities < 50%) within the perciform Aqp1aa subclusters. The tetrapod AQP1 and teleost Aqp1aa sequences clustered primarily according to phylogenetic rank wherein HhAqp1aa clustered with other pleuronectiform Aqp1aa orthologs. Such topologies imply minimal evolution of the encoded genes, a notion supported by the

comparatively short branch lengths and higher identity values to human AQP1. Although teleost Aqp1aa proteins show greater amino acid substitution (42%) compared to human AQP1, within Teleostei, the Aqp1aa primary structures are well conserved (86%) (table 1). By contrast the teleost Aqp1ab sequences did not cluster according to phylogenetic rank, but separated into three paralogous subclusters. HhAqp1ab is placed together with similar pleuronectiform and acanthomorph Aqp1ab sequences within subcluster 2, but is distinct from other acanthomorph Aqp1ab orthologs in subcluster 3. The divergent topology of the Aqp1ab sequences is also reflected in the separate clustering of the ostariophysan zebrafish in subcluster 3 compared to the ostariophysan catfishes in subcluster 1. Bayesian branch length values for both the codon and amino acid runs were on average 3.5 times longer for the teleost Aqp1ab sequences compared to the Aqp1aa orthologs and suggest that the Aqp1ab genes are rapidly diverging within the teleost crown clade. Inspection of the C-terminal domains revealed that significantly greater amino acid substitution has occurred within the Aqp1ab cytoplasmic region compared to either Aqp1aa, dipnoan Aqp1 or tetrapod AQP1 (table 1 and supplementary fig. S1, Supplementary Material online).

To test whether the C-terminal domains were responsible for the novel subclustering of the teleost Aqp1ab orthologs, separate Bayesian and maximum likelihood analyses were run on truncated alignments lacking the N- and C-termini. These new trees (data not shown) reflected the topology of the full length analyses, and reveal that significantly greater amino acid substitution occurs throughout the primary structures of the teleost Aqp1ab orthologs. Despite this divergence, three dimensional models of the halibut aquaporin paralogs indicate that the transmembrane helical topology is well conserved, whereas the C-termini are rapidly evolving even in closely related species (see supplementary fig. S1, Supplementary Material online).

An extended synteny analysis confirmed that teleost *aqp1aa* and *-1ab* genes are tandemly arranged in orthologous regions upstream of THO complex subunit 1 (*thoc1*) and downstream of corticotropin releasing hormone receptor 2 (*crhr2*) (fig. 2). The genomic regions are well conserved amongst the acanthomorph species (torafugu, green-spotted pufferfish, stickleback and medaka), while the flanking genes have experienced greater rearrangement in zebrafish. Interestingly the syntenic data show that the teleost *aqp1aa*, *-1ab* and flanking gene loci share greater homology to the genomic regions in the anole

lizard and birds. By contrast mammals have only retained syntenic loci for the closely linked G-protein coupled receptors (*CRHR2, GHRHR, ADCYAP1R1*), the neurogenic differentiation factor (*NEUROD6*), and the calmodulin-dependent phsophodiesterase (*PDE1C*). Within Eutheria, however, gene synteny flanking the AQP1 locus is in fact highly conserved. Consequently greater rearrangement of these genomic regions appears to have occurred in the mammalian lineage.

Taking into consideration the tandem arrangement of the teleost *aqp1aa* and *-1ab* genes, the highly conserved synteny within the acanthomorph genomes, and the close phylogenetic clustering of the halibut aquaporins with stickleback *aqp1aa* and *-1ab*, it seems likely that these aquaporin paralogs are tandem duplicates. This suggests that the WGD product (i.e. the true *aqp1b* gene) is lost in the Acanthomorpha. To confirm this notion, we examined the syntenic locus of the zebrafish *aqp5/1b* pseudogene. It is found at the 21.6 Mb locus on LG 3 between integrin alpha 2 (*ita2b*) and corticotropin releasing hormone receptor 1 (*crhr1*), but is also linked to the homeobox ba (*hoxba*) cluster and *aqp8b*. This genomic region is not conserved in the acanthomorph genomes, but is partially conserved in the anole lizard on LG 6 (63-64 Mb locus), the orthologon that retains AQP1 at 1.9 Mb. The acanthomorph *aqp8b* orthologs have, however, remained linked to the *hoxba* clusters on the respective LGs, while the *crhr1* genes are found on the sister paralogons linked to the *hoxbb* clusters and the *aqp8aa* and *-8ab* tandem duplicates. Based upon this evidence we conclude that the functional teleost *aqp1* paralogs (previously named *aqp1a* and *-1b*) are indeed tandem duplicates, and we therefore renamed these genes *aqp1aa* and *-1ab*, while the zebrafish pseudogene was renamed *aqp5/1b* to match the *aqp8* terminology.

HhAqp1aa and -1ab Are Differentially Expressed

hhaqp1aa and *-1ab* transcript abundance in different organs and tissues of adult Atlantic halibut was determined by qPCR (see supplementary fig. S2*A*, Supplementary Material online). *hhaqp1aa* mRNA was detected ubiquitously at comparable levels in all the tissues analyzed, with less expression in the esophagus, stomach, pyloric caeca, spleen and lens. In contrast, *hhaqp1ab* transcripts were found predominantly in the ovary, followed by testis, ureter, head kidney, rectum and eye, although transcripts could also be detected at much

lower levels in most of the other organs. Accumulation of *hhaqp1ab* in the ovary, however, was ~50-fold higher than in testis and ureter, ~600-fold higher than in head kidney, rectum and eye, and >1000-fold higher than in the rest of tissues analyzed.

Antibodies generated against the HhAqp1ab C-terminus specifically identified the protein in total membrane extracts from the ovary, testis, ureter, head kidney, rectum and eye (supplementary fig. S2*B*, Supplementary Material online). However, the amount of HhAqp1ab protein in the different tissues deduced from Western blotting analysis apparently did not correlate well with the amount of mRNA determined by qPCR in some cases. In addition, multiple HhAqp1ab immunoreactive bands with different molecular masses were observed in different tissues. In the ovary and testis, which differentially express *hhaqp1ab* by ~30-fold, the HhAqp1ab antiserum predominantly detected a ~27 kDa protein of similar intensity, which is near the HhAqp1ab predicted molecular mass (~28.4 kDa), (supplementary fig. S2*B*, arrows, Supplementary Material online). However, other polypeptides of ~50 kDa and ~66 kDa were also detected (supplementary fig. S2*B*, arrowheads, Supplementary Material online). In extracts from the head kidney, ureter and eye, the 27-kD protein band was not detected, but different immunoreactive polypeptides with molecular masses from ~39 to ~80 kDa, appearing as smeared or more defined bands, were observed. The 27-kD protein, and the other polypeptides of higher molecular mass, were no longer detected after pre-incubation of the HhAqp1ab antiserum with large amounts of the immunizing peptide (supplementary fig. S2*B*, right panel, Supplementary Material online), indicating that the high molecular weight bands correspond to post-translational modifications of HhAqp1ab. Such modifications do not appear to involve glycosylation because they were not sensitive to PNGase F or O-Glycosidase digestion (data not shown), but most likely represent HhAqp1ab oligomers that are stable under denaturing and reducing conditions, presumably due to the high hydrophobicity of the protein (Van Hoek et al. 1995). The formation of these complexes seems to be more prominent in the ureter.

HhAqp1ab is Functional Only When Expressed in Halibut Oocytes

To determine whether *hhaqp1aa* and *-1ab* cDNAs encoded functional water channels, *X. laevis* oocytes were injected *ex vivo* with *hhaqp1aa* or *-1ab* cRNAs or with water as

negative controls (fig. 3*A*-*E*). Oocytes expressing HhAqp1aa proteins showed a ~22-fold increase in P_f with respect to the control oocytes after an osmotic challenge, which was inhibited by 83% with mercury and partially reversed with β-mercaptoethanol, an observation consistent with the presence of Cys^{181} in HhAqp1aa (fig. 3*B*). In contrast, *X. laevis* oocytes expressing HhAqp1ab did not swell significantly more than the controls (fig. 3*B*), indicating that this paralog was not functional. However, when HhAqp1aa and -1ab were expressed *in vivo* in PV halibut oocytes (fig. 3*F*), both paralogs were functional resulting in ~17- and ~8-fold increase in P_f, respectively, compared to control oocytes (fig. 3*G*). As observed in the *ex vivo* experiments, mercury inhibited HhAqp1aa- and -1ab-mediated water transport by ~75%, the inhibition being partially recovered with β-mercaptoethanol (fig. 3*G*).

Immunofluorescence microscopy revealed that HhAqp1ab polypeptides were retained in the cytoplasm of *X. laevis* oocytes (fig. 3*C* and *D*), explaining the functional failure of HhAqp1ab, whereas in halibut oocytes the protein was readily targeted to the plasma membrane (fig. 3*H* and *I*). Immunoblotting analysis of total membrane protein extracts from *X. laevis* and halibut ovarian follicles expressing HhAqp1ab indicated the translation of HhAqp1ab monomers and the formation of ~50-kDa complexes in both oocytes. However, functional expression of HhAqp1ab and the formation of the 66-kDa complex was only detected *in vivo* in the halibut oocytes (fig. 3*E* and *J*). Interestingly, when HhAqp1ab was expressed in zebrafish oocytes, the protein was highly accumulated at the plasma membrane, and in this system both HhAqp1aa and -1ab elicited a similar ~6-fold increase in P_f after oocytes were exposed to a hyperosmotic medium (see supplementary fig. S3, Supplementary Material online).

To investigate whether the functional failure of HhAqp1ab in *X. laevis* oocytes was due to the expression system used, HhAqp1b was expressed in amphibian oocytes that were injected with $polyA^+$ mRNA purified from PV Atlantic halibut ovarian follicles (fig. 4). Injection of $polyA^+$ mRNA alone into oocytes resulted in a significant but moderate increase of P_f with respect to control oocytes and those expressing HhAqp1ab alone (1.6-fold), but when halibut $polyA^+$ mRNA was co-expressed with HhAqp1ab a synergistic effect was observed resulting in a marked increase (7.5-fold) of the P_f (fig. 4*A*). Exposure of $polyA^+$ mRNA plus HhAqp1ab-expressing oocytes to mercury inhibited water

permeability by 75%, and the inhibition was almost fully recovered with β-mercaptoethanol. Accordingly, immunolabeling of oocytes demonstrated that HhAqp1ab was translocated to the oocyte plasma membrane exclusively when it was co-expressed with polyA$^+$ mRNA from halibut ovarian follicles (fig. 4*B* and *C*). Western blotting after SDS-PAGE under reducing (fig. 4*D*) and non-reducing (data not shown) conditions indicated that the pattern of post-translational modifications of HhAqp1ab in oocytes was identical regardless of the expression of polyA$^+$ mRNA from ovarian follicles, but the 66-kDa HhAqp1ab complexes, previously observed in halibut oocytes, were only detected in the plasma membrane fraction (fig. 4*D*). These results thus indicated that *ex vivo* injection of polyA$^+$ mRNA from halibut follicles into *X. laevis* oocytes was able to reproduce the *in vivo* intracellular mechanisms for the insertion of HhAqp1ab into the plasma membrane. Injection of the HhAqp1ab antiserum into oocytes expressing mRNA and HhAqp1ab inhibited oocyte swelling in a dose-dependent manner up to 93% (fig. 4*E*), confirming that most of the water transport measured in these oocytes was mediated by HhAqp1ab. In accordance with the inhibition of oocyte P_f, the HhAqp1ab antiserum reduced the presence of the protein at the plasma membrane while its abundance in the total membrane fraction remained unchanged (fig. 4*F*). These observations suggest that the antibody most likely affects the turnover of HhAqp1ab in the oocyte plasma membrane.

In some teleosts, the intracellular trafficking of Aqp1ab is regulated by specific domains at the C-terminus of the protein (Tingaud-Sequeira et al. 2008; Chaube et al. 2011). Therefore, we next investigated the presence of similar domains in HhAqp1ab that might interact with factors encoded by mRNAs expressed in Atlantic halibut ovarian follicles. For these experiments, cDNAs encoding chimeric HhAqp1aa and -1ab proteins in which the N- and/or C-terminal domains were exchanged (HhAqp1aa-Nab, -Cab, -Nab-Cab, and HhAqp1ab-Naa, -Caa, -Naa-Caa) were synthesized *in vitro*. The chimeras and wild-type (WT) *hhaqp1aa* and *-1ab* were injected into oocytes, with or without polyA$^+$ mRNA from halibut ovarian follicles, and the P_f monitored (fig. 4*G*). Oocytes expressing HhAqp1aa-WT or -Nab showed the same P_f regardless of the presence of polyA$^+$ mRNA, although the HhAqp1aa-Nab oocytes significantly reduced swelling by 19% when compared with oocytes expressing HhAqp1aa-WT. In contrast, the permeability of HhAqp1aa-Cab and -Nab-Cab oocytes was strongly reduced (96%) in the absence of

polyA$^+$ mRNA, but the reduction was only 51% when these chimeras were co-expressed with polyA$^+$ mRNA from halibut follicles. As observed earlier, oocytes expressing HhAqp1ab showed a high increase in P_f in the presence of polyA$^+$ mRNA, but the substitution of the N-terminus of HhAqp1ab by that of HhAqp1aa had no effect. However, when the C-terminus of HhAqp1ab was exchanged with that of HhAqp1aa, or both N- and C-termini were substituted, a 2.6-fold increase of P_f was observed, which was not affected by the expression of halibut polyA$^+$ mRNA in the oocytes. These results therefore suggest that the halibut polyA$^+$ mRNA-derived mechanisms controlling the function of HhAqp1ab in oocytes primarily rely on the C-terminus of the protein.

Endogenous HhAqp1ab is Up-Regulated During Oocyte Hydration and Translocated into the Oocyte Plasma Membrane

To investigate the regulation of endogenous HhAqp1ab during *in vivo* oocyte hydration in Atlantic halibut, we determined changes in *hhaqp1ab* gene expression and protein synthesis in PV, EH, MH, and H ovarian follicles, as well as in unfertilized eggs, collected from reproductively active females. As it has been previously reported (Finn et al. 2002), halibut ovarian follicles undergoing meiotic maturation swell by a factor of ~4-fold, coincident with the fusion of yolk globules and progressive 'clearing' of the oocyte cytoplasm (fig. 5*A*-*E*; see also fig. 6*D*-*F*) as a result of alterations in the ultrastructure of crystalline inclusions of yolk globules (Selman et al. 2001; Fabra et al. 2006). This process renders a ~45% increase in water content in the oocyte (Finn et al. 2002). SDS-PAGE and Coomassie blue staining of Vtg-derived oocyte yolk proteins in extracts from follicle-enclosed oocytes confirmed the complete hydrolysis of the lipovitellin heavy chain of VtgAa (LvH-Aa), and the partial degradation of the lipovitellin light chain of VtgAb (LvL-Ab), during oocyte maturation and hydration (fig. 5*F*, arrows) described previously (Finn 2007a). Such massive hydrolysis contributes to most of the organic osmolyte pool of FAA that drives water uptake (Finn 2007a).

The qPCR analyses showed that follicular *hhaqp1ab* transcript levels steadily increase from PV to MH ovarian follicles (3.0 ± 0.19 units in MH, relative to PV follicles) (fig. 5*G*). However, in H follicles and eggs *hhaqp1ab* mRNA was largely degraded (0.55 ± 0.01 and 0.40 ± 0.07 units in H and eggs, respectively, relative to PV follicles). The amount

of HhAqp1ab monomer protein in the follicle determined by Western blotting notably followed that of its mRNA, progressively increasing from PV to H follicles (fig. 5*H*, arrow). Interestingly, the ~50-kDa post-translational modification of HhAqp1ab was noted only in PV follicles, whereas the 66-kDa complexes were detected exclusively in H follicles and eggs, being much more prominent in H follicles (fig. 5*H*, arrowheads).

Immunofluorescence and immunoelectron microscopy was subsequently carried out to investigate the subcellular localization of HhAqp1ab in PV, EH, MH and H follicles (fig. 6). In PV follicles, HhAqp1ab fluorescence and immunogold labeling was found exclusively within vesicles spread in the oocyte cytoplasm between the yolk globules (fig. 6*A,D,G* and *M*). As hydration commences in EH follicles, HhAqp1ab fluorescence was detected in the oocyte cytoplasm as well as in the most cortical region of the oocyte just below the plasma membrane (fig. 6*B,E* and *H*). When oocytes reached a more advanced stage of hydration in MH follicles, HhAqp1ab was localized exclusively within a thin region below the oocyte plasma membrane (fig. 6*C,F* and *I*). Immunogold analysis of H follicles containing almost or fully hydrated oocytes, revealed the presence of HhAqp1ab along the oocyte microvilli that traverse the vitelline envelope (fig. 6*N-P*). Altogether, these findings indicate that the sequential up-regulation of *hhaqp1ab* and its protein product occurring during meiotic maturation and oocyte hydration in Atlantic halibut is followed by the translocation of HhAqp1ab to the oocyte plasma membrane, where it forms non-reducible oligomeric complexes of about 66 kDa. These findings confirm the previous observations using *X. laevis* oocytes co-expressing *hhaqp1ab* cRNA and polyA$^+$ mRNA from halibut ovarian follicles.

Mercury Causes a Decrease in the Hydration of Halibut Follicle-Enclosed Oocytes

As a first approach to investigate the role of HhAqp1ab during oocyte hydration, we employed $HgCl_2$, since *in vivo* and *ex vivo* experiments showed that mercury was effective at inhibiting HhAqp1ab-mediated water transport. In these experiments, halibut EH follicles that had already initiated meiosis resumption and oocyte hydration *in vivo* were briefly exposed to increasing doses of $HgCl_2$ and subsequently treated with or without β-mercaptoethanol (supplementary fig. S4, Supplementary Material online). Treatment of follicles with mercury did not affect oocyte maturation or the hydrolysis of yolk proteins as

indicated by SDS-PAGE and Coomassie blue staining (supplementary fig. S4*A-F*, Supplementary Material online). However, follicles matured in the presence of 0.25, 0.5 or 1 mM $HgCl_2$ showed diminished oocyte hydration compared to untreated controls (supplementary fig. S4*A-E* and *G*, Supplementary Material online). Hydration inhibition was dose-dependent (28%, 36% and 50% using 0.25, 0.5 or 1 mM $HgCl_2$, respectively), and could be fully reversed with β-mercaptoethanol when follicles were exposed 0.25 mM $HgCl_2$, but only partially reversed when higher doses of mercury were used (supplementary fig. S4*G*, Supplementary Material online).

Inhibition of Oocyte Hydration with the HhAqp1ab Antibody is Rescued by Over-Expression of HhAqp1aa

Since it is known that mercury can affect other membrane proteins in addition to aquaporins, we investigated whether specific inhibition of HhAqp1ab was responsible for blocking oocyte hydration. For these experiments, we used the HhAqp1ab antiserum because this antibody was able to inhibit HhAqp1ab-mediated water transport in *X. laevis* oocytes. Follicle-enclosed EH oocytes were thus injected with the anti-HhAqp1ab antibody or rabbit IgG as a control, and subsequently placed in culture medium for 48 h to resume oocyte maturation and hydration *in vitro* (fig. 7). Injection of the HhAqp1ab antibody did not affect maturational proteolysis of yolk proteins (data not shown), but did inhibit oocyte hydration in a dose-dependent manner (fig. 7*A-F*). Relative to controls injected with PBS vehicle, hydration was inhibited by 27%, 46% and 60%, in oocytes injected with 100, 250 and 500 ng/oocyte of HhAqp1ab antiserum, respectively, whereas injection of IgG was ineffective (fig. 7*G*). To demonstrate that the reduction of oocyte hydration was caused by the specific inhibition of HhAqp1ab, oocytes injected with the anti-HhAqp1ab antiserum were co-injected with *hhaqp1aa* or *-1ab* cRNA and cultured up to 72 h. Over-expression of exogenous *hhaqp1ab* in oocytes partially recovered the inhibition of oocyte hydration caused by the antibody, whereas the expression of *hhaqp1aa*, the protein product of which is not recognized by the antibody (fig. 3*E*), was more effective and fully rescued the hydration of the oocytes (fig. 7*H-J*).

Immunoblotting analyses using anti-IgG and HhAqp1ab antibody directly coupled to HRP confirmed that increasing doses of the antibody were effectively injected into the

halibut oocytes. Further, the inhibition of oocyte hydration by the HhAqp1ab antiserum correlated with the disappearance of the 66-kDa HhAqp1ab complex, whereas the HhAqp1ab monomer was detected regardless of the treatment of oocytes (fig. 7*K*). In extracts from follicles injected with the HhAqp1ab antiserum and over-expressing HhAqp1ab the 66-kDa band could be detected again, suggesting that, as observed in *X. laevis* oocytes, the HhAqp1ab antibody most likely affected the turnover of HhAqp1ab in the plasma membrane of halibut oocytes.

These results support the conclusion that water transport through the tandemly duplicated HhAqp1ab paralog is required for full hydration of Atlantic halibut oocytes. Antibody-induced retention of HhAqp1ab inhibits this hydration, while yolk proteolysis and meiosis resumption in the oocyte is not affected.

Discussion

It is now well established that teleosts experienced a specific round of WGD at the root of the crown clade (Amores et al. 1998; Jaillon et al. 2004; Volff 2005; Crow et al. 2006). Indeed our previous analysis of the aquaporin superfamily in zebrafish revealed that WGD endowed teleosts with the largest repertoire of aquaporins in the vertebrate lineage (Tingaud-Sequeira et al. 2010). By re-examining the molecular phylogeny of the vertebrate aquaporin-1 subfamily, the present data reveal that tetrapod *AQP1* and teleost *aqp1aa* orthologs cluster according to phylogenetic rank and display significantly shorter branch lengths compared to the teleost *aqp1ab* orthologs. We show for the first time, however, that the latter *aqp1ab* transcripts and proteins separate into three sister clusters. If subcluster 1 and 2 are collated and compared to subcluster 3, the within cluster topologies also follow phylogenetic rank, with acanthomorph and ostariophysan sequences represented twice. Such paralogous topologies usually indicate the existence of two genes. To investigate this possibility, we conducted an extended synteny analysis of the vertebrate aquaporin-1 loci.

These data reveal that while synteny is highly conserved within the acanthomorph teleosts (medaka, stickleback, and the pufferfishes), it is less conserved when compared to zebrafish, a feature we have noted for other gene families (Finn et al. 2009; Cerdà and Finn 2010; Chauvigné et al. 2010). Nevertheless, the teleost-specific aquaporin paralogs (*aqp1aa*

and *-1ab*) are all tandemly arranged between *crhr2* and *thoc1*. The medaka is the only exception, which as noted previously (Tingaud-Sequeira et al. 2008), appears to have lost the *aqp1ab* paralog. An interesting aspect of this analysis is the more conserved gene contiguity between zebrafish and the Sauria, and the absence of syntenic conservation in the mammalian lineage. While it is known that teleost genomes have experienced WGD and subsequent rearrangements (Kasahara et al. 2007; Nakatani et al. 2007; Muffato and Roest-Crollius 2008), the higher conservation of synteny between teleostean, amphibian, reptilian and avian lineages suggests that the regional loss of synteny occurred within Mammalia. Within Eutheria, including the Primates (chimpanzee, gorilla, orangutan, macaque and marmoset), Glires (mouse, rat and rabbit), Lausiatheria (Cow and horse) and Afrotheria (elephant) synteny is highly conserved as indicated between humans and dogs. However, it is broken at the *THOC1* locus, in which the syntenic cassette of blue-annotated genes observed downstream of the *aqp1aa-aqp1ab-thoc1* loci in Teleostei is found on separate chromosomes (e.g. LG 18 in humans and LG 7 in dogs), an arrangement also true for all eutherian mammals. The same cassette of genes has also been rearranged in birds, but in zebra finch and the chicken they have remained linked on the same chromosomes (e.g. LG 2 in the zebra finch and chicken, respectively) and are thus not contiguous. In the turkey, and the anole lizard however, these genes have apparently relocated to LG 3 and LG 4, respectively. We conclude from this analysis that the aquaporin-1 loci are encoded in complex regions of vertebrate genomes that have undergone lineage-specific intra- and inter-chromosomal shuffling.

Importantly, the syntenic data show that the aquaporin-1 subfamily in teleosts reflects the *aqp8* system, in which WGD together with tandem duplication gave rise to *aqp8aa*, *aqp8ab* and *aqp8b* (Tingaud-Sequeira et al. 2010; Cerdà and Finn 2010). In the case of the teleost *aqp1* paralogs, *aqp1aa* and *-1ab* represent the tandem duplicates, while the WGD product (i.e. the true *aqp1b*) is probably lost in many species, but appears to exist in the zebrafish genome as the fused *aqp5/1b* pseudogene (Tingaud-Sequeira et al. 2010; Cerdà and Finn 2010). The co-clustering of *hhaqp1aa* and *-1ab* together with stickleback *aqp1aa* and *-1ab*, respectively, further implies that tandem duplication of an ancestral *aqp1* gene provided the likely basis for the adaptive evolution of the *aqp1ab* paralog.

An interesting aspect of this finding is the co-evolution of the organic osmolyte system that drives oocyte hydration in marine teleosts. Both the yolk precursor gene (*vtgaa*), which is highly expressed in marine teleost oocytes, and ultimately leads to the liberation of FAA in the maturing oocyte, and the water channel (*aqp1ab*) responsible for mediating water influx in a co-ordinated developmental process, appear to have arisen through tandem duplication rather than WGD (Finn et al. 2009; Finn and Fyhn 2010; Cerdà and Finn 2010). The subsequent neofunctionalization of the proteins reveals that gene duplication *per se* is an important foundation of novel cellular pathways that alter the phenotype. In the latter instance, it is the rise of the pelagic egg, which we suggest had broad implications for the oceanic radiation of teleosts (Finn and Kristoffersen 2007; Kristoffersen et al. 2009).

Tandem duplication is not unique to the teleost *aqp1aa* and *-1ab* orthologs. In humans, our synteny analysis reveals a putative *AQP1*-like paralog at the 30.9 Mb locus on LG 7, two genes upstream of the conserved *AQP1* locus. Similarly, *AQP7* and *AQP12* appear to have tandemly duplicated in some Primates, while in teleosts, the *Aqp8* genes have also tandemly duplicated to give rise to *aqp8aa* and *aqp8ab* in addition to the WGD product, *aqp8b* (Tingaud-Sequeira et al. 2010; Cerdà and Finn 2010). For teleosts, however, it is the tandemly duplicated *aqp8aa* and *aqp1ab* genes that have neofunctionalized. We show here through molecular phylogeny and functional assays that the C-terminus of Aqp1ab is the most rapidly evolving aquaporin subdomain in the vertebrate lineage. Within each group, tetrapod AQP1 and teleost Aqp1aa have undergone similar rates of amino acid substitution (13-17%), while the duplicated Aqp1ab paralog has experienced significantly greater amino acid substitution, particularly within the C-terminal domain. Given that Tetrapoda and Teleostei evolved over similar timescales (~390 million years), the present data provide an eminent example of primary structural divergence in the aftermath of gene duplication.

Neofunctionalization of the *aqp1ab* paralog is further indicated by the more restricted tissue expression pattern. Within Tetrapoda, *AQP1* is expressed in a wide range of tissues (King et al. 2004; Takata et al. 2004), a semi-ubiquitous pattern also noted for *hhaqp1aa* and other teleost *aqp1aa* transcripts (Cerdà and Finn 2010). By contrast *hhaqp1ab* is highly expressed in the ovary, but can also be found at lower levels in the testis, kidney and ureter,

observations that further concur with data for other teleosts (Cerdà and Finn 2010; Sun et al. 2010; Tipsmark et al. 2010). The qPCR data for *hhaqp1ab*, however, show that a specific up-regulation occurs during meiosis resumption, but ceases at the H oocyte stage. These data correlate very well with the transient hyperosmolality of the halibut ooplasm in relation to the ovarian fluid, due in part to ion accumulation and yolk proteolysis (Finn et al. 2002). The current data further show that increased accumulation of *hhaqp1ab* transcripts occurs during the maximal phase of yolk proteolysis. The subsequent *in vivo* increase of the HhAqp1ab protein in hydrating/hydrated oocytes, and its localization in the microvillar portion of the plasma membrane, further explain the ensuing increase in oocyte size associated with water influx and consequently the decrease in intra-oocytic osmolality (Finn et al. 2002).

As expected from previous studies in teleosts (Fabra et al. 2005; Tingaud-Sequeira et al. 2008; Kagawa et al. 2009; Tingaud-Sequeira et al. 2010), and the structural features of HhAqp1ab, $HgCl_2$ was able to reversibly block HhAqp1ab permeability when expressed in both homologous and heterologous oocytes, as well as to reduce the hydration normally associated with the meiotic maturation of Atlantic halibut oocytes. However, because mercury is not a specific aquaporin blocker, and may affect ion channels involved in the oocyte hydration mechanism (Cerdà et al. 2007; Cerdà 2009; Finn and Fyhn 2010), we tested for a more specific inhibition of HhAqp1ab function by using the HhAqp1ab antisera raised against the C-terminus of the protein. This antisera proved effective at blocking the translocation of HhAqp1ab into the oocyte plasma membrane. Microinjection of the antibody in halibut oocytes resulted in a dose-dependant inhibition of oocyte hydration, while the process of yolk hydrolysis and meiotic maturation were not affected. The immunological inhibition could be fully reversed by the artificial expression of HhAqp1aa, which is functional in halibut oocytes, but is not recognized by the antibody. Consequently, the decrease of hydration of halibut oocytes can be directly related to the loss of function of HhAqp1ab. These findings, together with the gene expression and cellular localization data, therefore provide for the first time functional evidence of the essential role of Aqp1ab-mediated water transport during the hydration of fish oocytes undergoing meiotic maturation.

Despite the high level of amino acid substitution within the teleost Aqp1ab orthologs, its role during oocyte hydration is most likely conserved in marine species (Tingaud-Sequeira et al. 2008; Cerdà 2009). Part of the explanation underlying this phenomenon may be due to functional constraints in the endocrine pathways that control nuclear and cytoplasmic maturation in addition to oocyte hydration. One such example is a report showing convergent evolution of genes encoding the luteinizing hormone receptor (*lhcgrb*) in Teleostei (Chauvigné et al. 2010). Nevertheless, HhAqp1ab seems to be an unusually highly specialized aquaporin since we found that this protein did not traffic to the oocyte plasma membrane unless it is expressed in native or piscine oocytes. As a molecular phylogenetic member of the Aqp1ab subcluster (2), HhAqp1ab is thus unlike the closely related Senegalese sole (*Solea senegalensis*) Aqp1ab or the more distantly related gilthead seabream ortholog in subcluster (3), or stinging catfish and European eel Aqp1ab channels in subcluster (1), that are functional in heterologous systems such as amphibian oocytes (Tingaud-Sequeira et al. 2008; Chaube et al. 2011). This is surprising given that, to our knowledge, AQP12 orthologs are the only vertebrate aquaporins that are not targeted to the plasma membrane when expressed in *X. laevis* oocytes, a feature that has been explained by the intracellular localization of this aquaporin in pancreatic acinar cells (Itoh et al. 2005; Ohta et al. 2009). The *ex vivo* functional failure of HhAqp1ab in *X. laevis* oocytes could not be alleviated by exposure of oocytes to known signal transduction molecules such as cAMP or cGMP (data not shown), that are known to control trafficking of catfish Aqp1ab as well as of tetrapod AQP2 and AQP-h2 (Hasegawa et al. 2003; Nedvetsky et al. 2009; Chaube et al. 2011). While these results suggest that phosphorylation might not play a role in the plasma membrane localization of HhAqp1ab, its function during HhAqp1ab trafficking can not be ruled out due to the highly divergent nature of the putative phosphorylation sites within the teleost Aqp1ab C-termini (see supplementary fig. S1, Supplementary Material online). Indeed, phosphorylation of Ser^{254} has been shown to mediate Aqp1ab recycling in the gilthead seabream (Tingaud-Sequeira et al. 2008). Interestingly, however, by co-expressing HhAqp1ab cRNAs with $polyA^+$ mRNA purified from PV Atlantic halibut ovarian follicles in *X. laevis* oocytes, it was possible to rescue the *ex vivo* membrane trafficking of HhAqp1ab. These observations suggest that HhAqp1ab and halibut oocytes may have co-evolved lineage-specific, protein-based mechanisms for the intracellular

transport of HhAqp1ab during meiotic maturation. In support of this hypothesis is the observation that HhAqp1ab was fully functional when expressed in oocytes of a distantly related ostariophysan teleost such as the zebrafish.

The precise nature of the polyA$^+$ mRNA-derived mechanism controlling HhAqp1ab plasma membrane localization in oocytes is yet unknown. Our present data reveal however that the HhAqp1ab C-terminus is likely involved, as indicated by functional experiments using wild-type HhAqp1aa and -1ab and chimeric constructs. This finding reinforces the role of the C-terminus in the rapid neofunctionalization of Aqp1ab among teleosts, but the specific function of this domain in the trafficking mechanism of HhAqp1ab remains intriguing. In addition to phosphorylation, C-terminus-mediated interactions with cytoskeletal components, sorting vesicles and lysosomal trafficking regulators (Kamsteeg et al. 2007; Nedvetsky et al. 2009; Moeller et al. 2010), as well as proper folding of the proteins in the endoplasmic reticulum (ER) (van Balkom et al. 2002; Pitonzo and Skach 2006), can control the intracellular transport of aquaporins. In the present study, post-translational modifications of HhAqp1ab resulting from the co-expression of polyA$^+$ mRNA from Atlantic halibut oocytes were not evident by Western blotting analysis of total membrane extracts from *X. laevis* oocytes under reducing or non-reducing conditions. This suggests that HhAqp1ab was properly folded and not retained in the ER even in the absence of polyA$^+$ mRNA from halibut oocytes. Under such conditions, i.e. retention in the ER, aquaporins are usually glycosylated (Deen et al. 1995) and our data indicate that HhAqp1ab is not glycosylated. However, translocation of functional HhAqp1ab into the oocyte plasma membrane was associated with the formation of a 66-kDa HhAqp1ab complex in both native Atlantic halibut oocytes undergoing hydration as well as in *X. laevis* oocytes co-expressing HhAqp1ab and polyA$^+$ mRNA. These complexes most likely represent strong HhAqp1ab oligomers that do not dissociate under denaturing and reducing conditions, as found for the *Escherichia coli* AqpZ (Borgnia et al. 1999) and some plant aquaporins (Ohshima et al. 2001; Casado-Vela et al. 2010). Therefore, whether the enzymatic machinery for the formation of these complexes is only present in teleost oocytes, and/or is a highly specific sorting mechanism of Aqp1ab-containing vesicles that is absent in *X. laevis* oocytes, remains to be investigated.

In conclusion, by using Atlantic halibut as a model species with large oocytes and a reproductive strategy adapted to low temperatures, we provide direct functional evidence for the essential and conserved physiological role of the tandemly duplicated Aqp1ab paralog during meiosis resumption in marine teleosts. The data show that the rapid divergence of the C-terminal domain of HhAqp1ab results in *ex vivo* loss of function in amphibian oocytes, which can be rescued by injection of polyA$^+$ mRNA from native Atlantic halibut oocytes. These findings thus reveal the dual nature of neofunctionalization of the teleost Aqp1ab water channels where selection pressure has favoured oocyte hydration, but has been relaxed with regard to the specific cellular mechanisms controlling membrane trafficking.

Acknowledgments

This work was supported by Grants from the Spanish Ministry of Science and Innovation (MICINN; AGL2007-60261/ACU) and European Commission (MRTN-CT-2006-035995-Aquaglyceroporins) to JC, and by a Grant from the Research Council of Norway (204813) to RNF. CZ and FC were supported by predoctoral (FPI) and postdoctoral (Juan de la Cierva Programme) fellowships, respectively, from MICINN. We thank S. O. Utskot and the staff at Austevoll Research Station for expert help in sampling the Atlantic halibut, and N. Cortadellas and A. García for their excellent technical support for electron microscopy.

References

Amores A, Force A, Yan YL, et al. (13 co-authors) 1998. Zebrafish *hox* clusters and vertebrate genome evolution. *Science* 282:1711-1714.

Armstrong CM. 1990. Potassium channel architecture and channel blockers. *Prog Clin Biol Res.* 334:1-15.

Blom N, Gammeltoft S, Brunak S. 1999. Sequence and structure-based prediction of eukaryotic protein phosphorylation sites. *J Mol Biol*. 294:1351-1362.

Blom N, Sicheritz-Pontén T, Gupta R, Gammeltoft S, Brunak S. 2004. Prediction of post-translational glycosylation and phosphorylation of proteins from the amino acid sequence. *Proteomics* 4:1633-1649.

Borgnia MJ, Kozono D, Calamita G, Maloney PC, Agre P. 1999. Functional reconstitution and characterization of AqpZ, the *E. coli* water channel protein. *J Mol Biol.* 291:1169-1179.

Casado-Vela J, Muries B, Carvajal M, Iloro I, Elortza F, Martínez-Ballesta MC. 2010. Analysis of root plasma membrane aquaporins from *Brassica oleracea*: post-translational modifications, de novo sequencing and detection of isoforms by high resolution mass spectrometry. *J Proteome Res*. 9:3479-3494.

Cerdà J, Fabra M, Raldúa D. 2007. Physiological and molecular basis of fish oocyte hydration. In: Babin PJ, Cerdà J, Lubzens, editors. The Fish Oocyte: From Basic Studies to Biotechnological Applications. Dordrecht: Springer. p. 349-396.

Cerdà J. 2009. Molecular pathways during marine fish egg hydration: the role of aquaporins. *J Fish Biol*. 75:2175-2196.

Cerdà J, Finn RN. 2010. Piscine aquaporins: An overview of recent advances. *J Exp Zool*. 313A:623-650.

Chaube R, Chauvigné F, Tingaud-Sequeira A, Joy KP, Acharjee A, Singh V, Cerdà J. 2011. Molecular and functional characterization of catfish (*Heteropneustes fossilis*) aquaporin-1b: changes in expression during ovarian development and hormone-induced follicular maturation. *Gen Comp Endocrinol*. 170:162-171.

Chauvigné F, Tingaud-Sequeira A, Agulleiro MJ, Calusinska M, Gómez A, Finn RN, Cerdà J. 2010. Functional and evolutionary analysis of flatfish gonadotropin receptors reveals cladal- and lineage-level divergence of the teleost glycoprotein receptor family. *Biol Reprod.* 82:1088-1102.

Crow KD, Stadler PF, Lynch VJ, Amemiya C, Wagner GP. 2006. The "fish-specific" Hox cluster duplication is coincident with the origin of teleosts. *Mol Biol Evol.* 23:121-136.

Deen PMT, Verdijk MAJ, Knoers N, Wieringa B, Monnens LA, van Os CH, van Oost BA. 1994. Requirement of human renal water channel aquaporin-2 for vasopressin-dependent concentration of urine. *Science* 264:92-95.

Deen PM, Croes H, van Aubel RA, Ginsel LA, van Os CH. 1995. Water channels encoded by mutant aquaporin-2 genes in nephrogenic diabetes insipidus are impaired in their cellular routing. *J Clin Invest*. 95:2291-2296.

Eppig JJ, Viveiros MM, Marin-Bivens C, de La Fuente R. 2004. Regulation of mammalian oocyte maturation. In: Leung PCK, Adashi EY, editors. The Ovary, 2nd edition. San Diego: Elsevier/Academic Press. p. 113-129.

Fabra M, Raldúa D, Power DM, Deen PM, Cerdà J. 2005. Marine fish egg hydration is aquaporin-mediated. *Science* 307:545.

Fabra M, Raldúa D, Bozzo MG, Deen PM, Lubzens E, Cerdà, J. 2006. Yolk proteolysis and aquaporin-1o play essential roles to regulate fish oocyte hydration during meiosis resumption. *Dev Biol.* 295:250-262.

Finn RN. 2007a. The maturational disassembly and differential proteolysis of paralogous vitellogenins in a marine pelagophil teleost: a conserved mechanism of oocyte hydration. *Biol Reprod*. 76:936-948.

Finn RN. 2007b. Vertebrate yolk complexes and the functional implications of phosvitins and other subdomains in vitellogenins. *Biol Reprod*. 76:926-935.

Finn RN, Kristoffersen BA. 2007. Vertebrate vitellogenin gene duplication in relation to the "3R hypothesis": correlation to the pelagic egg and the oceanic radiation of teleosts. *PLoS One* 2:e169.

Finn RN, Fyhn HJ. 2010. Requirement for amino acids in ontogeny of fish. *Aquaculture Res*. 41:684-716.

Finn RN, Østby GC, Norberg B, Fyhn HJ. 2002. *In vivo* oocyte hydration in Atlantic halibut (*Hippoglossus hippoglossus*): proteolytic liberation of free amino acids, and ion transport, are driving forces for osmotic water influx. *J Exp Biol*. 205:211-224.

Finn RN, Kolarevic J, Kongshaug H, Nilsen F. 2009. Evolution and differential expression of a vertebrate vitellogenin gene cluster. *BMC Evol Biol*. 9:2.

Fulton TW. 1898. On the growth and maturation of the ovarian eggs of teleostean fishes. *Fish Board Scotland, 16th Ann. Rep.*, Part 3:83-134.

Fyhn HJ, Finn RN, Reith M, Norberg B. 1999. Yolk protein hydrolysis and oocyte free amino acids as key features in the adaptive evolution of teleost fishes to seawater. *Sarsia* 84:451-456.

Greeley MSJr, Calder DR, Wallace RA. 1991. Changes in size hydration and low molecular weight osmotic effectors during meiotic maturation of *Fundulus* oocytes in vivo. Comp Biochem Physiol. 100A:639-674.

Hasegawa T, Tanii H, Suzuki M, Tanaka S. 2003. Regulation of water absorption in the frog skins by two vasotocin-dependent water-channel aquaporins, AQPh2 and AQP-h3. *Endocrinology* 144:4087-4096.

Hirano Y, Okimoto N, Kadohira I, Suematsu M, Yasuoka K, Yasui M. 2010. Molecular mechanisms of how mercury inhibits water permeation through aquaporin-1: understanding by molecular dynamics simulation. *Biophys J.* 98:1512-1519.

Itoh T, Rai T, Kuwahara M, Ko SB, Uchida S, Sasaki S, Ishibashi K. 2005. Identification of a novel aquaporin, AQP12, expressed in pancreatic acinar cells. *Biochem Biophys Res Commun*. 330:832-838.

Jacoby SC, Gagnon E, Caron L, Chang J, Isenring P. 1999. Inhibition of Na(+)-K(+)-2Cl(-) cotransport by mercury. *Am J Physiol*. 277:C684-C692.

Jaillon O, Aury JM, Brunet F, et al. (61 co-authors) 2004. Genome duplication in the teleost fish *Tetraodon nigroviridis* reveals the early vertebrate proto-karyotype. *Nature* 431:946–957.

Kagawa H, Horiuchi Y, Kasuga Y, Kishi T. 2009. Oocyte hydration in the Japanese eel (*Anguilla japonica*) during meiosis resumption and ovulation. *J Exp Zool Ecol Genet Physiol*. 311A:752-762.

Kamsteeg EJ, Deen PM. 2001. Detection of aquaporin-2 in the plasma membranes of oocytes: a novel isolation method with improved yield and purity. *Biochem Biophys Res Commun*. 282:683-690.

Kamsteeg EJ, Duffield AS, Konings IBM, Spencer J, Pagel P, Deen PMT, Caplan MJ. 2007. MAL decreases the internalization of the aquaporin-2 water channel. *Proc Natl Acad Sci USA* 104:16696-16701.

Kasahara M, Naruse K, Sasaki S, et al. (38 co-authors) 2007. The medaka draft genome and insights into vertebrate genome evolution. *Nature* 447:14-719.

King LS, Kozono D, Agre P. 2004. From structure to disease: the evolving tale of aquaporin biology. *Nat Rev Mol Cell Biol.* 5:687-698.

Kolarevic J, Nerland A, Nilsen F, Finn RN. 2008. Goldsinny wrasse (*Ctenolabrus rupestris*) is an extreme vtgAa-type pelagophil teleost. *Mol Reprod Dev*. 75:1011-1020.

Kristoffersean BA, Finn, RN. 2008. Major osmolyte changes during oocyte hydration of a clupeocephalan marine benthophil: Atlantic herring. *Mar Biol.* 154:683-692.

Kristoffersen BA, Nerland A, Nilsen F, Kolarevic J, Finn RN. 2009. Genomic and proteomic analyses reveal non-neofunctionalized vitellogenins in a basal clupeocephalan, the Atlantic herring, and point to the origin of maturational yolk proteolysis in marine teleosts. *Mol Biol Evol*. 26:1029-1044.

Laemmli, UK. 1970. Cleavage of structural proteins during the assembly of the head of bacteriophage T4. *Nature* 227:680-685.

Lessman CA. 2009. Oocyte maturation: converting the zebrafish oocyte to the fertilizable egg. *Gen Comp Endocrinol*. 161:53-57.

Livak KJ, Schmittgen TD. 2001. Analysis of relative gene expression data using real-time quantitative PCR and the 2(-Delta Delta C(T)) method. *Methods* 25:402-408.

Moeller HB, Praetorius J, Rützler MR, Fenton, R.A. 2010. Phosphorylation of aquaporin-2 regulates its endocytosis and protein-protein interactions. *Proc Natl Acad Sci USA* 107:424-429.

Muffato M, Roest Crollius H. 2008. Paleogenomics in vertebrates, or the recovery of lost genomes from the mist of time. *BioEssays* 30:122-134.

Nagahama Y, Yamashita M. 2008. Regulation of oocyte maturation in fish. *Dev. Growth Differ.* 50 (Suppl. 1):S195-S219.

Nakatani Y, Takeda H, Kohara Y, Morishita S. 2007. Reconstruction of the vertebrate ancestral genome reveals dynamic genome reorganization in early vertebrates. *Genome Res*. 17:1254-1265.

Nedvetsky PI, Tamma G, Beulshausen S, Valenti G, Rosenthal W, Klussmann E. 2009. Regulation of aquaporin-2 trafficking. *Handb Exp Pharmacol*. 190:133-157.

Norberg B, Valkner V, Huse J, Karlsen I, Grung GL. 1991. Ovulatory Rhythms and egg viability in the Atlantic halibut (*Hippoglossus hippoglossus*). *Aquaculture* 97:365-371.

Notredame C, Higgins DG, Heringa J. 2000. T-Coffee: A novel method for fast and accurate multiple sequence alignment. *J Mol Biol*. 302:205-217.

Ohshima Y, Iwasaki I, Suga S, Murakami M, Inoue K, Maeshima M. 2001. Low aquaporin content and low osmotic water permeability of the plasma and vacuolar membranes of a CAM plant *Graptopetalum paraguayense*: comparison with radish. *Plant Cell Physiol*. 42:1119-1129.

Ohta E, Itoh T, Nemoto T, et al. (13 co-authors) 2009. Pancreas-specific aquaporin 12 null mice showed increased susceptibility to caerulein-induced acute pancreatitis. *Am J Physiol Cell Physiol*. 297:C1368-C1378.

Philpott A, Yew PR. 2008. The *Xenopus* cell cycle: an overview. *Mol Biotechnol*. 39:9-19.

Pitonzo D, Skach WR. 2006. Molecular mechanisms of aquaporin biogenesis by the endoplasmic reticulum Sec61 translocon. *Biochim Biophys Acta*. 1758:976-988.

Preston GM, Jung JS, Guggino WB, Agre P. 1993. The mercury-sensitive residue at cysteine 189 in the CHIP28 water channel. *J Biol Chem*. 268:17-20.

Selman K, Wallace RA. 1986. Gametogenesis in *Fundulus heteroclitus*. *Am Zool* 26:173-192.

Selman K, Wallace RA, Cerdà J. 2001. Bafilomycin A1 inhibits proteolytic cleavage and hydration but not yolk crystal disassembly or meiosis during maturation of sea bass oocytes. *J Exp Zool* 290:265-278.

Sun Y, Zhang Q, Qi J, Yu Y, Li S, Li C, Zhong Q. 2009. Cloning, expression and analysis of two Aquaporin-1 paralogous genes in *Cynoglossus semilaevis*. *J Wuhan University* (Natural Science Edition) 55:335-339 (in Chinese with English summary).

Sun Y, Zhang Q, Qi J, Chen Y, Zhong Q, Li C, Yu Y, Li S, Wang Z. 2010. Identification of differential genes in the ovary relative to the testis and their expression patterns in half-smooth tongue sole (*Cynoglossus semilaevis*). *J Genet Genomics* 37:137-145.

Suyama M, Torrents D, Bork P. 2006. PAL2NAL: robust conversion of protein sequence alignments into the corresponding codon alignments. *Nucleic Acids Res*. 34:W609-W612.

Takata K, Matsuzaki T, Tajika Y. 2004. Aquaporins: water channel proteins of the cell membrane. *Prog Histochem Cytochem*. 39:1-83.

Thomas P, Tubbs C, Berg H, Dressing G. 2007. Sex steroid hormone receptors in fish ovaries. In: Babin PJ, Cerdà J, Lubzens E, editors. The Fish Oocyte: From Basic Studies to Biotechnological Applications. Dordrecht: Springer. p. 203-233.

Tingaud-Sequeira A, Chauvigné F, Fabra M, Lozano J, Raldúa D, Cerdà J. 2008. Structural and functional divergence of two fish aquaporin-1 water channels following teleost-specific gene duplication. *BMC Evol Biol*. 8:259.

Tingaud-Sequeira A, Calusinska M, Finn RN, Chauvigné F, Lozano J, Cerdà J. 2010. The zebrafish genome encodes the largest vertebrate repertoire of functional aquaporins with dual paralogy and substrate specificities similar to mammals. *BMC Evol Biol*. 10:38.

Tipsmark CK, Sørensen KJ, Madsen SS. 2010. Aquaporin expression dynamics in osmoregulatory tissues of Atlantic salmon during smoltification and seawater acclimation. *J Exp Biol*. 213:368-379.

van Balkom BW, Savelkoul PJ, Markovich D, Hofman E, Nielsen S, van der Sluijs P, Deen PM. 2002. The role of putative phosphorylation sites in the targeting and shuttling of the aquaporin-2 water channel. *J Biol Chem*. 277:41473-41479.

Van Hoek AN, Wiener MC, Verbavatz JM, Brown D, Lipniunas PH, Townsend RR, Verkman AS. 1995. Purification and structure-function analysis of native, PNGase, F-treated and endo-beta-galactosidase-treated CHIP28 water channels. *Biochemistry* 34:2212-2219.

Volff JN. 2005. Genome evolution and biodiversity in teleost fish. *Heredity* 94:280-294.

Westerfield M. 1995. The zebrafish book. 2nd edition. Oregon: University of Oregon Press.

Figure legends

FIG. 1. Maximum likelihood tree of orthologous vertebrate aquaporin-1 codons rooted with inshore hagfish aquaporin 4. The Atlantic halibut sequences cloned in the present study are indicated by thick black arrows. Three sister clusters (sarcopterygian *AQP1*, and teleost *aqp1aa* and *aqp1ab*) are indicated by black circles at the relevant nodes, while three novel subclusters (1-3) are indicated for the *aqp1ab* orthologs. The teleost-specific whole genome duplication (WGD) event is indicated by a black triangle, while tandem duplication is indicated by a black square. Statistical values at each node represent Bayesian posterior probabilities resulting from 5 million MCMC generations of full-length codon/amino acid alignments. Polytomies in the protein trees are annotated with (-). Scale bar represents the rate of nucleotide substitution per site.

FIG. 2. Genomic synteny of vertebrate aquaporin-1 orthologs. Linkage groups (LG) are drawn to scale on the left, illustrating the loci of the conserved aquaporin-1 genes shown in the main panel. Red numbers in parentheses represent the length of the analyzed regions in megabases (Mb), and show that mammalian regions are more expanded (7.2-10.3 Mb) compared to birds (3.6-4.8 Mb) and Teleostei (0.6-3.1 Mb). Gene coding direction is indicated by the pointed end of each symbol. A circular arrow to the left of a given region indicates that it is flipped. Syntenic loci that are conserved between tetrapods and teleosts (e.g. *CRHR2*, *AQP1*, *GHRHR*, *ADCYAP1R1*, *NEUROD6*, *PDE1C*) are annotated in black with black linker lines. Closely linked gene loci that are conserved between mammals, birds, the anole lizard and the Western-clawed frog are annotated in grey with grey linker lines. Gene loci that are syntenic between birds, the anole lizard, the Western-clawed frog and teleosts are annotated in green with green linker lines, while syntenic genes specific to the teleost regions are annotated in blue with blue linker lines. Pale blue symbols without linker lines represent non-syntenic genes.

FIG. 3. HhAqp1ab, but not HhAqp1aa, is functional only when expressed *in vivo* in Atlantic halibut oocytes. (*A, F*) Photomicrographs of a *X. laevis* stage V oocyte (A) and of a halibut PV ovarian follicle (F). (*B, G*) Osmotic water permeability (P_f ± SEM of 3-4 independent experiments; n = 40-45 oocytes) of *X. laevis* (*B*) and halibut (*G*) oocytes injected with water (control) or with 1 or 25 ng cRNA encoding HhAqp1aa and -1ab, respectively, and treated with or without 0.3 mM $HgCl_2$ and 5 mM β-mercaptoethanol (ME). An asterisk indicates a significant increase in P_f compared to control and $HgCl_2$-treated oocytes ($P < 0.01$). (*C, D, H, I*) The HhAqp1ab is retained in the ooplasm (O) of *X. laevis* oocytes (*C, D*) but translocated into the plasma membrane (arrows) when expressed in

halibut oocytes (*H, I*). Paraffin sections of water- and HhAqp1ab-injected oocytes probed with the HhAqp1ab antiserum followed by FITC anti-rabbit IgG. Arrowheads point to the microvilli crossing the vitelline envelope (VE). Scale bars: 25 μm (*C, D*); 10 μm *(H, I*). (*E, J*) Immunoblots of total membranes of *X. laevis* (*E*; 0.5 oocyte equivalent/lane) and halibut (*J*; 2 oocyte equivalent/lane) using the HhAqp1ab antiserum of oocytes that were used for the P_f measurements. The arrows indicate HhAqp1ab monomers, whereas the arrowheads points to possible post-translational modifications of HhAqp1ab. Molecular mass markers (kDa) are on the left.

FIG. 4. *Ex vivo* translocation of HhAqp1ab requires its C-terminus and polyA$^+$ mRNA from halibut oocytes. (*A*) P_f (mean ± SEM of 4 independent experiments; n = 30-45 oocytes) of *X. laevis* oocytes injected with water, polyA$^+$ mRNA purified from halibut PV ovarian follicles, HhAqp1ab alone, or polyA$^+$ mRNA plus HhAqp1ab. Oocytes injected with polyA$^+$ mRNA and HhAqp1ab were treated with mercury and β-mercaptoethanol as in Fig. 3. Values with a different superscript are significantly different (ANOVA, $P < 0.05$). (*B-C*) HhAqp1ab is translocated into the plasma membrane in the presence of polyA$^+$ mRNA. The arrows point to the plasma membrane. Bars, 15 μm. (*D*) Immunoblots of total membranes (TM; 0.5 oocyte equivalent/lane) or purified plasma membranes (PM; 3 oocyte equivalent/lane), using the HhAqp1ab antiserum, of *X. laevis* oocytes used in A. HhAqp1ab monomers and potential post-translational modifications are indicated as in Fig. 3. Molecular mass markers (kDa) are on the left. (*E*) Percentage inhibition of P_f (mean ± SEM of 2 independent experiments; n = 30-32 oocytes) of *X. laevis* oocytes expressing HhAqp1ab in the presence of polyA$^+$ mRNA and injected with increasing amounts of the HhAqp1ab antiserum or rabbit IgG (controls). The asterisks indicate significant differences (Student *t*-test, $P < 0.01$) at each antibody concentration. (*F*) Immunoblot of total and plasma membranes of oocytes showed in *E*. (*G*) P_f (mean ± SEM of 3 independent experiments; n = 40-50 oocytes) of oocytes expressing cRNA encoding wild-type (WT) HhAqp1aa or -1ab, or chimeric proteins in which the N- and C-terminus were exchanged, in the presence or absence of polyA$^+$ mRNA from halibut follicles. Values with different superscript are significantly different (ANOVA, $P < 0.05$).

FIG. 5. *hhaqp1ab* and its protein product are sequentially up-regulated during Atlantic halibut oocyte hydration. (*A-E*) Photomicrographs of isolated Atlantic halibut ovarian follicles undergoing oocyte hydration *in vivo*. PV, postvitellogenic follicle; EH, early hydrating follicle; MH, mid-hydrated follicle; H, hydrated follicle; Egg, unfertilized egg. Scale bar: 1 mm. (*F*) Changes of major yolk proteins of halibut follicles (0.02 follicle equivalents/lane) during hydration resolved by 12% SDS-PAGE and further staining with Coomassie blue R-350. The arrows indicate proteolysis of

VtgAa lipovitellin heavy chain and VtgAb lipovitellin light chain (LvH-Aa and LvL-Ab, respectively) during oocyte hydration. Molecular mass markers (kDa) are on the left. (*G*) *hhaqp1ab* expression levels in halibut ovarian follicles during oocyte hydration as determined by qPCR. Transcript levels of *18s* were used as reference, and relative transcript levels (mean ± SEM; $n = 3$ cDNAs from a pool from 3-4 females) were calculated as fold change with respect the PV follicles. Values with different superscript are significantly different (ANOVA, $P < 0.05$). (*H*) Representative HhAqp1ab immunoblot of total membranes from halibut ovarian follicles (5 follicle equivalents/lane). The arrow indicates HhAqp1ab monomers, whereas the arrowheads points to possible post-translational modifications of HhAqp1ab. Molecular mass markers (kDa) are on the left.

FIG. 6. HhAqp1ab is translocated to the microvillar membranes of Atlantic halibut oocytes during hydration. (*A-F*) Plastic sections of PV (*A, D*), EH (*B, E*) and MH (*C, F*) ovarian follicles stained with methylene blue (which stains yolk) showing the process of yolk globule fusion and disassembly in the oocyte during hydration. Scale bars: 1 mm (*A-C*); 50 µm (*D-F*). (*G-L*) Immunofluorescence microscopy for HhAqp1ab on the same stage ovarian follicles revealed that HhAqp1ab (arrows) is translocated from the ooplasm towards the periphery of the oocyte during hydration. Control sections (*J-L*) were incubated with preabsorbed HhAqp1ab antiserum. Sections were counterstained with DAPI. Scale bars: 50 µm. (*M-P*) Immunoelectron microscopy micrographs of PV and H ovarian follicles using the HhAqp1ab antiserum. In PV follicles (*M*), immunogold particles (arrows) are localized exclusively within vesicles spread in the ooplasm, whereas in H follicles (*N-P*) HhAqp1ab gold particles become apparent in the microvilli extending from the oocyte through the vitelline envelope. Scale bars: 0.25 µm (*M, N*); 0.20 µm (*O, P*). FC, follicle cells; MV, microvilli; TC, theca cells; VE, vitelline envelope; VS, vesicle; YG, yolk globule; O, ooplasm.

FIG. 7. Inhibition of oocyte hydration *in vitro* by injection of follicle-enclosed oocytes with the HhAqp1ab antiserum, and recovery by over-expression of HhAqp1aa. (*A-F*) Photomicrographs of Atlantic halibut EH ovarian follicles before (*A*) and after 48 h of injection with PBS (*B*), 500 ng rabbit IgG (*C*), or 100 (*D*), 250 (*E*) or 500 ng (*F*) of HhAqp1ab antiserum. Scale bar: 1 mm. (*G*) Inhibition of oocyte hydration (mean ± SEM of three independent experiments; $n = 45$ follicles) with 100, 250 and 500 ng of HhAqp1ab antiserum by 27.5 ± 2.2%, 46.5 ± 1.6%, and 60.5 ± 1.4%, respectively (asterisks denote significant differences at $P < 0.01$). (*H, I*) Photomicrographs of halibut follicles injected with 200 ng HhAqp1ab antiserum and 25 ng *hhaqp1aa* or *-1ab* cRNA after

72 h of culture. Scale bar: 1 mm. (*J*) Inhibition of oocyte hydration (mean ± SEM of four independent experiments; $n = 60$ follicles) with injection of 200 ng of rabbit IgG or HhAqp1ab antiserum, and partial or full recovery by co-injection with 25 ng of *hhaqp1ab* and *-1aa* cRNA, respectively. Values with different superscript are significantly different (ANOVA, $P < 0.01$). (*K*) Representative immunoblots for rabbit IgG (left) or HhAqp1ab (right) of whole homogenates or total membrane extracts, respectively (5 follicle equivalents/lane), from follicles injected with IgG or HhAqpa1b antiserum, and over-expressing or not *hhaqp1ab* or *-1aa* cRNAs. Membranes were probed only with HRP anti-rabbit IgG or with the HhAqp1ab antiserum labelled with HRP. Arrows indicate the heavy (HC) and light (LC) chains of IgG, and the HhAqp1ab monomers, whereas the arrowheads indicate potential post-translational modifications of HhAqp1ab. Molecular mass markers (kDa) are on the left.

Supplementary Data

Supplementary Table S1. List of accession numbers used for molecular phylogenetic inference.

Supplementary Table S2. N- and C-terminal amino acid sequences of HhAqp1aa and -1ab wild-type (WT) and chimeric proteins.

Supplementary Figure S1. Structural features of vertebrate aquaporin-1 orthologs.

Supplementary Figure S2. *hhaqp1aa* and *-1ab* are differentially expressed in Atlantic halibut adult tissues.

Supplementary Figure S3. Functional expression of HhAqp1aa and -1ab in zebrafish oocytes.

Supplementary Figure S4. Atlantic halibut oocyte hydration *in vitro* is inhibited by exposure of follicle-enclosed oocytes to $HgCl_2$.

Table 1. Group-wise amino acid (AA) sequence identity values (%) of vertebrate aquaporin-1 proteins. Analyses were conducted for full-length alignments, truncated alignments without the C-terminal domain and only the C-terminal domain. *N* represents the number of taxa included in each comparison. Postscripted numbers in parentheses refer to a given Aqp1ab subcluster shown in Fig. 1. Data are presented as means ± standard deviation.

Group	Cluster	*N*	Full-length	Full-length - C terminus	C terminus
AA identity *vs* Human AQP1			(300)	(246)	(54)
Tetrapoda	AQP1	12	83 ± 6.0 [a]	83 ± 5.8 [a]	87 ± 7.7 [a]
Dipnoi	Aqp1	1	64	66	54
Teleostei	Aqp1aa	20	58 ± 1.12 [b]	62 ± 1.1 [b]	39 ± 3.1 [b]
	Aqp1ab (3)	6	53 ± 2.2 [c]	58 ± 2.6 [c]	24 ± 4.2 [c]
	Aqp1ab (2)	4	48 ± 0.2 [d]	56 ± 0.4 [c]	11 ± 3.0 [d]
	Aqp1ab (1)	3	50 ± 2.2 [cd]	56 ± 2.0 [c]	20 ± 5.0 [c]
AA identity *vs* HhAqp1aa			(292)	(238)	(54)
Teleostei	Aqp1aa	19	86 ± 4.8 [a]	87 ± 4.5 [a]	79 ± 8.8 [a]
	Aqp1ab (3)	6	63 ± 4.8 [b]	70 ± 4.5 [b]	23 ± 5.6 [b]
	Aqp1ab (2)	4	55 ± 1.4 [c]	64 ± 2.2 [c]	12 ± 4.0 [c]
	Aqp1ab (1)	3	59 ± 3.9 [bc]	67 ± 3.5 [bc]	22 ± 6.1 [bc]

NOTE: Parenthetic numbers indicate the length of the alignments, including gaps. Significant differences are analyzed by ANOVA and indicated by non-equivalent superscripts.

0.2

Human *AQP1*
Mouse *AQP1*
Dog *AQP1*
Armadillo *AQP1*
Opossum *AQP1*
Platypus *AQP1*
Anole lizard *AQP1*
Chicken *AQP1*
Turkey *AQP1*
Common quail *AQP1*
House sparrow *AQP1*
Zebra finch *AQP1*
Mallard duck *AQP1*
Southern gray treefrog *AQP1*
Japanese treefrog *AQP1*
Marine toad *AQP1*
African lungfish *aqp1*

Mammalia
Lepidosauria
Aves
Amphibia
Dipnoi

AQP1

Sarcopterygii

Actinopterygii

Torafugu *aqp1aa*
G-S pufferfish *aqp1aa*
Common mummichog *aqp1aa*
Mi-iuy croaker *aqp1aa*
European seabass *aqp1aa*
Yellow perch *aqp1aa*
Grass rockfish *aqp1aa*
Atlantic toothfish *aqp1aa*
Gilthead seabream *aqp1aa*
Black porgy *aqp1aa*
Black seabass *aqp1aa*
Stickleback *aqp1aa*
Atlantic halibut *aqp1aa*
Japanese flounder *aqp1aa*
Senegalese sole *aqp1aa*
Half-smooth tongue sole *aqp1aa*
Medaka *aqp1aa*
Nile tilapia *aqp1aa*
Atlantic cod *aqp1aa*
Rainbow smelt *aqp1aa*
Rainbow trout *aqp1aa1*
Atlantic salmon *aqp1aa1*
Rainbow trout *aqp1aa2*
Atlantic salmon *aqp1aa2*
Northern pike *aqp1aa*
Fathead minnow *aqp1aa*
Zebrafish *aqp1aa*
Japanese eel *aqp1aa1*
Japanese eel *aqp1aa2*
European eel *aqp1aa*

Acanthomorpha
Protacanthopterygii
Neognathi
Ostariophysi
Elopomorpha

aqp1aa

Inshore hagfish *aqp4*

WGD
tandem duplication

Torafugu *aqp1ab*
G-S pufferfish *aqp1ab*
Gilthead seabream *aqp1ab*
Nile tilapia *aqp1ab*
Sockeye salmon *aqp1ab*
Atlantic salmon *aqp1ab*
Zebrafish *aqp1ab*
Atlantic halibut *aqp1ab*
Senegalese sole *aqp1ab*
Half-smooth tongue sole *aqp1ab*
Stickleback *aqp1ab*
Northern bluefin tuna *aqp1ab*
Channel catfish *aqp1ab*
Stinging catfish *aqp1ab*
European eel *aqp1ab*

Acanthomorpha
Protacanthopterygii
Ostariophysi
Acanthomorpha
Ostariophysi
Elopomorpha

aqp1ab

Zebrafish *aqp5/1b*

Ostariophysi

aqp1b

AQP1 loci

(27.2 - 37.8) Mb

(43.3 - 51.8)

(10.1 - 17.3)

(5.6 - 0.8)

(0.3 - 3.9)

(0.6 - 3.5)

(0.8 - 3.9)

(0.02 - 1.2)

(1.2 - 0.6)

(1.0 - 1.6)

(14.1 - 13.0)

(28.5 - 30.7)

(1.7 - 4.8)

LG 7 — Human

14 — Dog

Un — Opossum

2 — Zebra finch

2 — Chicken

6 — Turkey

6 — Anole lizard

Sca 333 — WC frog

Sca 68 — Torafugu

15r — GS pufferfish

III — Stickleback

17 — Medaka

2 — Zebrafish

Acanthomorpha

zebrafish

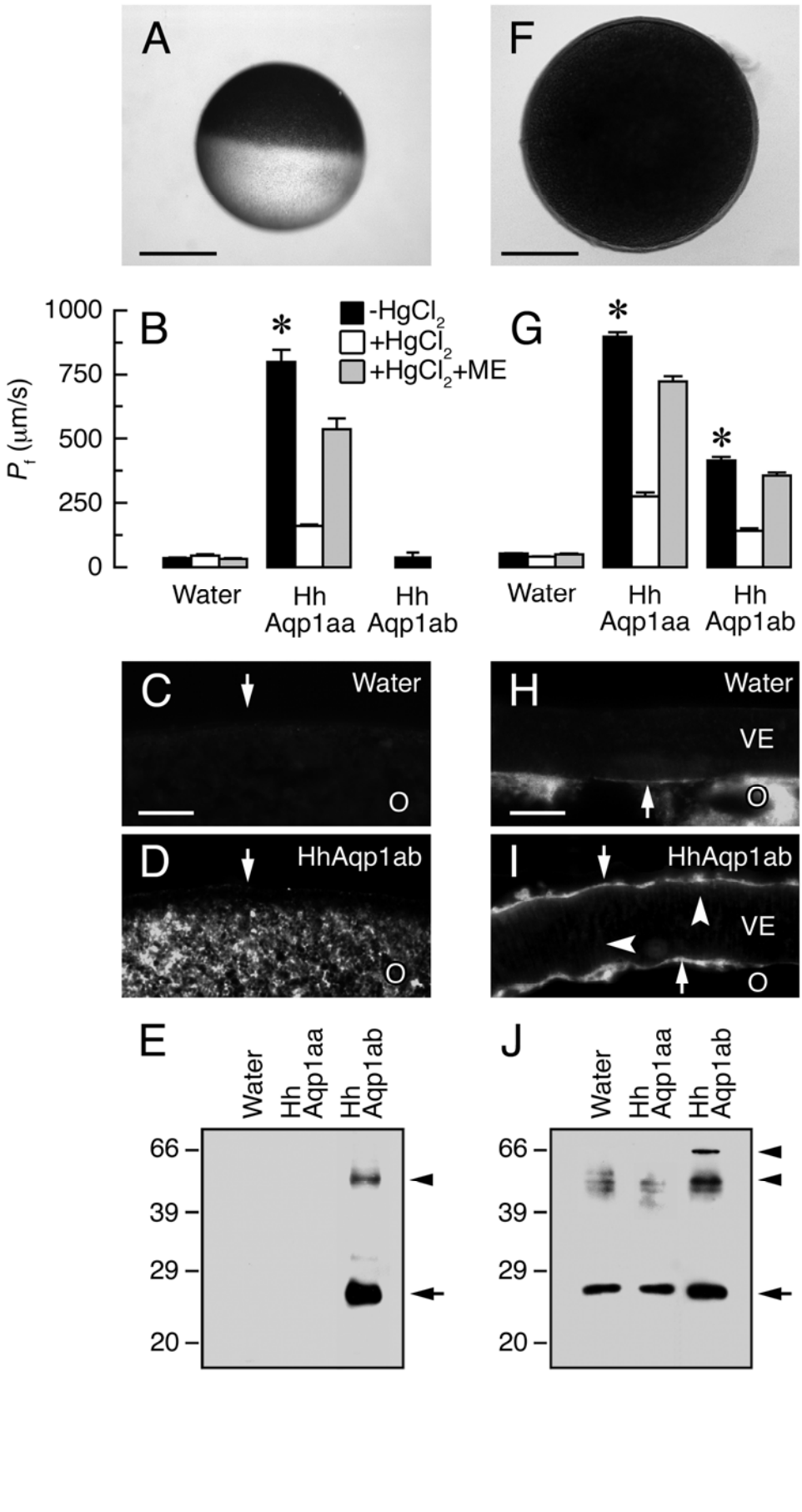
A
F
B
G
1000
750
500
250
0
P_f (μm/s)
-HgCl$_2$
+HgCl$_2$
+HgCl$_2$+ME
*
Water
Hh Aqp1aa
Hh Aqp1ab
C
H
Water
VE
O
D
I
HhAqp1ab
E
J
66
39
29
20

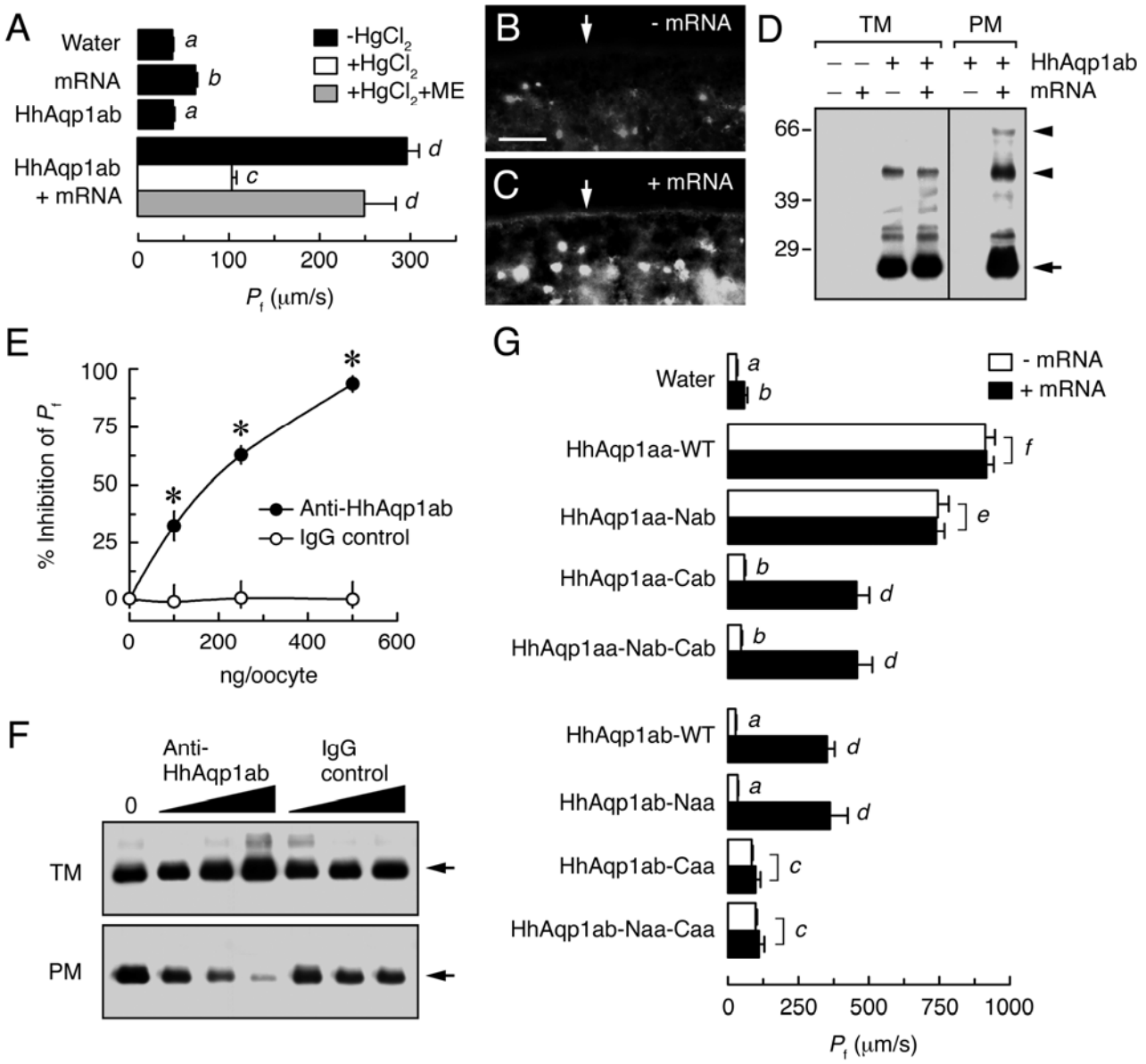
A
Water
mRNA
HhAqp1ab
HhAqp1ab + mRNA
-HgCl2
+HgCl2
+HgCl2+ME
a
b
a
d
c
d
0
100
200
300
Pf (μm/s)
B
- mRNA
C
+ mRNA
D
TM
PM
HhAqp1ab
mRNA
66
39
29
E
% Inhibition of Pf
Anti-HhAqp1ab
IgG control
ng/oocyte
F
Anti-HhAqp1ab
IgG control
TM
PM
G
- mRNA
+ mRNA
Water
HhAqp1aa-WT
HhAqp1aa-Nab
HhAqp1aa-Cab
HhAqp1aa-Nab-Cab
HhAqp1ab-WT
HhAqp1ab-Naa
HhAqp1ab-Caa
HhAqp1ab-Naa-Caa
0
250
500
750
1000
Pf (μm/s)

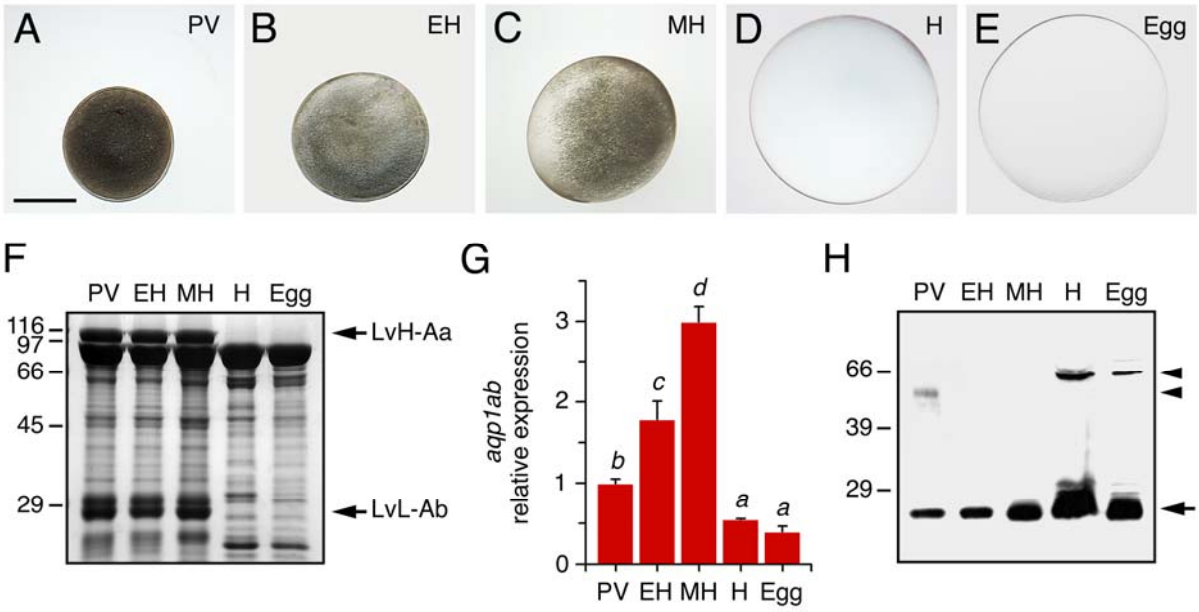
A
PV
B
EH
C
MH
D
H
E
Egg
F
PV EH MH H Egg
116
97
66
45
29
LvH-Aa
LvL-Ab
G
aqp1ab
relative expression
3
2
1
0
b
c
d
a
a
PV EH MH H Egg
H
PV EH MH H Egg
66
39
29

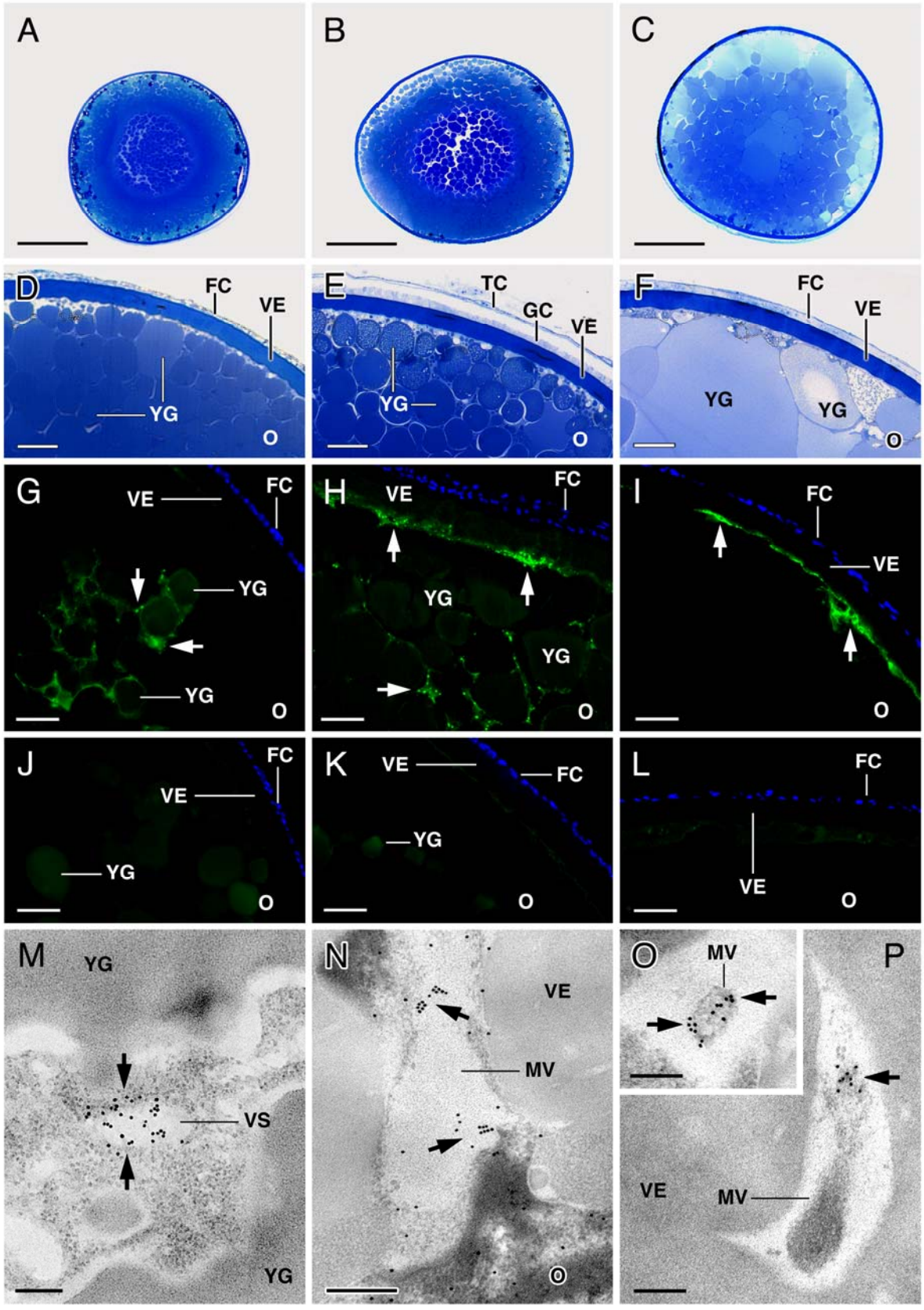
A
B
C
D
FC
VE
YG
O
E
TC
GC
VE
YG
O
F
FC
VE
YG
YG
O
G
VE
FC
YG
YG
O
H
VE
FC
YG
YG
O
I
FC
VE
O
J
FC
VE
YG
O
K
VE
FC
YG
O
L
FC
VE
O
M
YG
VS
YG
N
VE
MV
O
O
MV
P
VE
MV

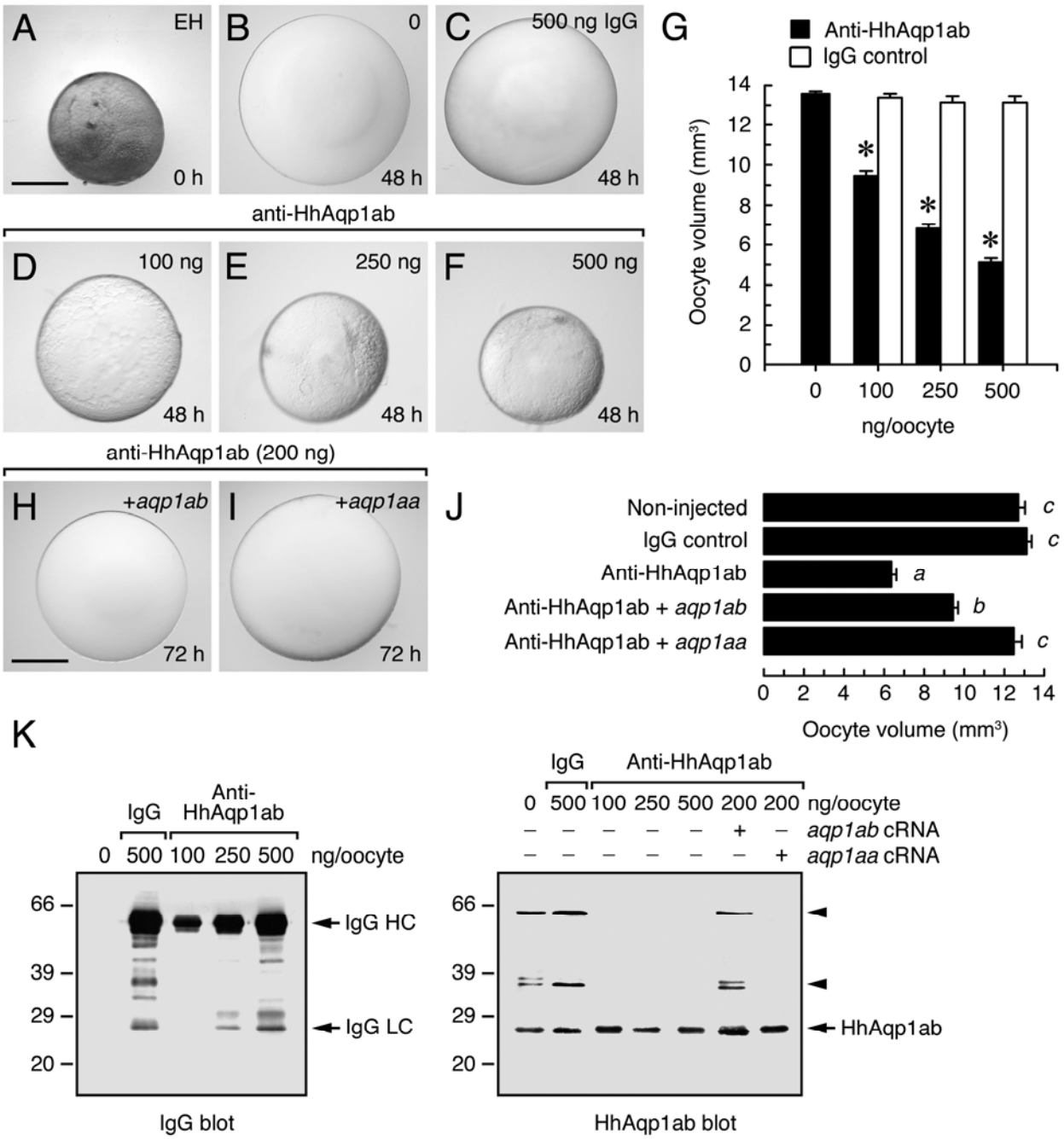
A
EH
0 h
B
0
48 h
C
500 ng IgG
48 h
anti-HhAqp1ab
D
100 ng
48 h
E
250 ng
48 h
F
500 ng
48 h
anti-HhAqp1ab (200 ng)
H
+aqp1ab
72 h
I
+aqp1aa
72 h
G
Anti-HhAqp1ab
IgG control
Oocyte volume (mm³)
ng/oocyte
J
Non-injected
IgG control
Anti-HhAqp1ab
Anti-HhAqp1ab + aqp1ab
Anti-HhAqp1ab + aqp1aa
Oocyte volume (mm³)
K
IgG
Anti-HhAqp1ab
0 500 100 250 500 ng/oocyte
IgG HC
IgG LC
IgG blot
0 500 100 250 500 200 200 ng/oocyte
aqp1ab cRNA
aqp1aa cRNA
HhAqp1ab
HhAqp1ab blot